Transcriptomic and functional analysis of *ANGPTL4* overexpression in pancreatic cancer nominates targets that reverse chemoresistance

Authors: Emily R. Gordon[1], Carter A. Wright[1,2], Mikayla James[1], Sara J. Cooper[1*]

Affiliations:

[1]HudsonAlpha Institute for Biotechnology, 601 Genome Way, Huntsville, AL 35806

[2]The University of Alabama in Huntsville, 301 Sparkman Drive, Huntsville, AL 35899

*Corresponding Author:

Sara J. Cooper

HudsonAlpha Institute for Biotechnology, 601 Genome Way

Huntsville, AL 35806, USA

Email: sjcooper@hudsonalpha.org

phone: 256-327-9491

ORCID: 0000-0002-9627-0309

ABSTRACT

Background

Pancreatic ductal adenocarcinoma (PDAC) is one of the deadliest cancers based on five-year survival rates. Genes contributing to chemoresistance represent novel therapeutic targets that can improve treatment response. Increased expression of *ANGPTL4* in tumors correlates with poor outcomes in pancreatic cancer.

Methods

We used statistical analysis of publicly available gene expression data (TCGA-PAAD) to test whether expression of *ANGPTL4* and its downstream targets, ITGB*4* and *APOL1*, were correlated with patient survival. We measured the impact of *ANGPTL4* overexpression in a common pancreatic cancer cell line, MIA PaCa-2 cells, using CRISPRa for overexpression and DsiRNA for knockdown. We characterized global gene expression changes associated with high levels of *ANGPTL4* and response to gemcitabine treatment using RNA-sequencing. Gemcitabine dose response curves were calculated on modified cell lines by measuring cell viability with CellTiter-Glo (Promega). Impacts on cell migration were measured using a time course scratch assay.

Results

We show that *ANGPTL4* overexpression leads to *in vitro* resistance to gemcitabine and reduced survival times in patients. Overexpression of *ANGPTL4* induces transcriptional signatures of tumor invasion and metastasis, proliferation and differentiation, and inhibition of apoptosis. Analyses revealed an overlapping signature of genes associated with both *ANGPTL4* activation and gemcitabine response. Increased expression of the genes in this signature in patient PDAC tissues was significantly associated with shorter patient survival. We identified 42 genes that were both co-regulated with *ANGPTL4* and were responsive to gemcitabine treatment. *ITGB4* and *APOL1* were among these genes. Knockdown of either of these genes in cell lines overexpressing *ANGPTL4* reversed the

observed gemcitabine resistance and inhibited cellular migration associated with epithelial to mesenchymal transition (EMT) and *ANGPTL4* overexpression.

Conclusions

These data suggest that *ANGPTL4* promotes EMT and regulates the genes *APOL1* and *ITGB4*. Importantly, we show that inhibition of both targets reverses chemoresistance and decreases migratory potential. Our findings have revealed a novel pathway regulating tumor response to treatment and suggest relevant therapeutic targets in pancreatic cancer.

KEYWORDS

ANGPTL4, APOL1, ITGB4, gemcitabine, chemoresistance, pancreatic cancer, PDAC, EMT, transcriptomic analysis, TCGA

BACKGROUND

Pancreatic ductal adenocarcinoma (PDAC) is among the deadliest cancers with a five-year survival of only 11% (SEER) **[1]**. The high mortality of pancreatic cancer patients is explained by the lack of early diagnostic markers leading to late-stage diagnosis of the disease and the high rate of treatment resistance **[2]**. Standard of care includes resection for about 20% of patients with localized disease who are eligible and treatment with cytotoxic chemotherapies such as gemcitabine or combination agents like FOLFIRINOX

69 (5-FU, oxaliplatin, folinic acid, and irinotecan). This combination, when tolerated,
70 improves progression-free survival by 11 months **[3]**. Despite the aggressive treatment
71 of this disease with combinations of cytotoxic drugs, the vast majority of patients do not
72 have an enduring response to the treatment. Through improvements in precision cancer
73 treatments based on genetic mutations, implementation of combination therapies like
74 FOLFIRINOX, and advances in immunotherapy over the last decade the five-year survival
75 has increased from 6% to 11%, nevertheless, pancreatic cancer remains extremely
76 deadly. These factors combined with the increased incidence of risk factors like diabetes
77 and obesity. It is predicted that pancreatic cancer will be the second leading cause of
78 cancer deaths by 2030 **[4]**.
79
80 Doubling the five-year survival rate is remarkable progress, but novel treatment strategies
81 are still needed. One effective strategy is to identify cellular markers or pathways that are
82 enriched in pancreatic cancer cells. For example, over 90% of PDAC tumors have a
83 mutation in the KRAS gene, however, no KRAS targeting treatments are available and
84 existing targeted therapies like PARP inhibitors **[5]** and EGFR inhibitors **[6]** are limited to
85 a subset of patients. It is clear that targeted therapies are impactful for the eligible patients
86 with significant improvement in progression-free survival among patients receiving a
87 targeted treatment **[7]**. Unfortunately, patients who do not respond to standard
88 chemotherapeutics and are not eligible for existing targeted therapies are left with few
89 options. Thus, there is significant interest in understanding the development of resistance,
90 and in pursuing targets that might sensitize resistant cells to existing treatments.
91

92 Our previous transcriptomic study identified genes whose expression was positively or
93 negatively correlated with patient survival and also linked to *in vitro* response to
94 gemcitabine, a common PDAC treatment. We identified ANGPTL4 among those genes
95 whose expression in patient tumors is associated with poor survival and whose
96 knockdown in PDAC cell lines could increase sensitivity to gemcitabine **[8]**. ANGPTL4 is
97 a member of the family of angiopoietin-like proteins that were first described for their role
98 in angiogenesis **[9, 10]**. ANGPTL4 can be proteolytically cleaved **[11]** and the two
99 products each have their own functions. The N-terminal domain plays a role in lipid
100 metabolism and genetic variation in this domain is linked to cardiovascular disease risk.
101 The C-terminal domain has been implicated in tumorigenesis, the promotion of
102 proliferation, and wound healing **[11, 12, 13]**.
103
104 Overall, the role of ANGPTL4 in cardiovascular disease and lipid metabolism has been
105 much better described than its roles in cancer. ANGPTL4 has a described role in known
106 cancer pathways including its ability to regulate CREB, FOS, and STAT3 via ERK
107 signaling **[14, 15]**. ANGPTL4's ability to alter metabolism and ATP abundance can also
108 impact drug transport **[15]**. The picture, however, is not perfectly clear since ANGPTL4
109 expression seems to have different impacts in cancers of different primary sites. For
110 example, methylation and downregulation of ANGPTL4 are associated with progression
111 and metastasis in colon cancer **[16]** but overexpression is associated with progression
112 and poor prognosis in breast cancer **[17]**. Breast cancers of the triple negative subtype
113 may be different since ANGPTL4 overexpression in that context has been associated with
114 inhibition of invasion **[18]**. In pancreatic cancer, *ANGPTL4* overexpression has been

115 associated with tumorigenesis **[19]**, cellular resistance to chemotherapy **[8]**, hypoxia
116 response, and poor patient outcomes **[20]**. The complicated role for ANGPTL4 motivates
117 our further exploration of its function in pancreatic cancer.
118
119 Here, we describe the role of ANGPTL4's in PDAC by exploring the molecular and cellular
120 changes associated with altered activity of ANGPTL4, the impact of ANGPTL4 on
121 chemoresistance, and the potential for inhibiting downstream pathways driven by
122 ANGPTL4 activation to sensitize tumor cells to treatment. We show that overexpression
123 of *ANGPTL4* leads to chemoresistance, increased migratory potential, and proliferation.
124 Our transcriptomic analysis revealed altered gene expression signatures downstream of
125 *ANGPTL4* overexpression that are linked to epithelial to mesenchymal transition (EMT)
126 and predict patient outcomes. We showed that knockdown of downstream effectors
127 including APOL1 and ITGB4 reversed resistance to treatment and reduced migratory
128 potential. The expression of these genes is also associated with patient survival. These
129 data support the hypothesis that ANGPTL4 and its downstream pathways are potential
130 therapeutic targets for the reversal of treatment resistance in pancreatic cancer.
131
132
133 **METHODS**
134 **Cell Culture**
135 HEK293FT cells (ThermoFisher #70007), MIA PaCa-2 cells (ATCC #CRM-CRL-1420),
136 and Panc-1 (ATCC #CRL-1469) were cultured in D10 media: DMEM (Lonza #12-614Q)
137 supplemented with 10% FBS, and 0.5% Penicillin-Streptomycin. All cell lines were

138 maintained at 37 °C and 5% CO_2. Cells were cryopreserved with the addition of 10%
139 DMSO (EMD #MX1458-6) to D10 media.
140
141 **Plasmids**
142 LentiSAMv2 (Addgene #92062) and lenti-MS2-p65-HSF1-Hygro (Addgene #89308) were
143 used to generate stable cell lines for gene activation. pMD2.G (Addgene #12259) and
144 psPAX2 (Addgene #12260) were used to facilitate viral packaging of sgRNA vector
145 plasmids.
146
147 **sgRNA Cloning**
148 sgRNA oligos were designed and cloned into their respective plasmids as described
149 previously (ANGPTL4: 5'-CACGGCCCTGGGGATGCCAAACTGTGG-3' and NTC: 5'-
150 ACGGAGGCTAAGCGTCGCAA-3') **[21]**.
151
152 **DsiRNA**
153 IDT TriFECTa RNAi kit was used per manufacturer's protocol. The DsiRNA sequences
154 used were as follows: ANGPTL4 (IDT hs.Ri.ANGPTL4.13.1), APOL1 (IDT
155 hs.Ri.APOL1.13.3), and ITGB4 (IDT hs.Ri.ITGB4.13.3). 100,000 cells were seeded per
156 well of a 12 well tissue culture treated plate 24 hours prior to transfection. Cells were
157 transfected using RNAiMax (ThermoFisher #13778-030) following manufacturer's
158 recommended protocol. As directed in the TriFecta kit (IDT #hs.Ri.HDAC1.13), TYE 563
159 transfection efficiency control, positive HPRT-S1 control, and negative (DS NC1)
160 scrambled sequence control were utilized. Functional assays were performed 48 hours

161 after transfection. Expression was validated with each transfection with IDT PrimeTime
162 qPCR Assay system according to manufacturer's recommendations on an Agilent
163 QuantStudio 6 Flex Real-Time PCR system (ANGPTL4: Hs.PT.58.40146104, ACTB:
164 Hs.PT.39a.22214847, GAPDH: Hs.PT.39a.22214836, and HPRT:
165 Hs.PT.58v.45621572).
166

167 **Protein Quantification using AlphaLISA**

168 Briefly, cells were seeded at 25,000 cells in 50uL of media per well of a 96-well tissue-
169 culture treated plate in triplicate per cell type. The following day, the media from each well
170 was transferred to a non-treated 96-well plate and 25ul of AlphaLISA Lysis Buffer
171 (PerkinElmer, #AL001C) was added per well. Plates were then shaken at 250 RPM at
172 room temperature for 10 minutes. Lysates were immediately used. Samples or standards
173 were transferred to a 384 well AlphaPlate (PerkinElmer, #600535, lot:8220-21331) and
174 the AlphaLISA ANGPTL4 manufacturer's kit protocol (PerkinElmer, #AL3017HV,
175 lot:2905318) was followed for standards, lysate, and supernatant (media) except for the
176 following: lids were covered in foil to prevent light exposure when possible and during
177 incubation periods plates were shaken at 150 RPM for the recommended time. The
178 AlphaLISA plate was read on a BioTek Synergy H5 following previously published
179 protocols **[22]**. Data were analyzed in R (version 4.1.2) and GraphPad Prism 9.
180

181 **RNA-sequencing**

182 Cells were seeded at a density of 0.6x10^6 cells per well of a 6-well plate in triplicate. The
183 following day media was removed and 3ml of media per well with or without 1.5nM of

184 gemcitabine (Sigma #G6423) was added and incubated for 24 hours. Media was
185 removed, cells were washed with PBS (Gibco #10010072), and released from the plate
186 with 2 ml of TrypLE (Gibco #12604-021) per well. After centrifugation, pellets were frozen
187 at -80C until RNA extraction. For RNA extraction, of cell pellets 350 ul of RL Buffer plus
188 1% BME from the Norgen Total RNA extraction kit and extraction proceeded per
189 manufacturer's instructions including use of the DNase kit (Norgen # 37500, 25720). RNA
190 quality was verified with the Agilent BioAnalyzer RNA Nano 600 kit (cat# 5067-1512) with
191 the RIN range between 9.2-10. RNA-sequencing libraries were made using Lexogen
192 QuantSeq 3' mRNA-Seq Library Prep Kit FWD for Illumina kit (cat# 015.24) with 250 ng
193 of RNA input. They were pooled and sequenced on an Illumina NextSeq 500 instrument
194 with 75 bp single-end reads. Read counts averaged 4 million reads and 93.65% of bases
195 exceeding Q30. Lexogen's BlueBee integrated QuantSeq data analyses pipeline was
196 used for trimming, mapping, and alignment and DESeq2 was used for differential
197 expression **[23]**. Heatmaps were generated using iDEP.95 **[24]**.
198

199 **Scratch-wound Assay**

200 Cells were seeded at 100,000 cells per well of a 96-well plate. After 24 hours uniform
201 scratches were made across the diameter of the wells using a multichannel pipette with
202 200ul pipette tips and even pressure applied across the wells to cause a wound. The
203 media was then vacuumed off and 200ul of new media was added. Cells were imaged on
204 a Lionheart FX Automated Microscope every 8 hours for 48 hours. Cell culture growth
205 conditions of 37 °C and 5% CO_2 were maintained throughout. Forty images were taken of
206 each scratch (4 wide by 10 long) with no overlap, autofocus, and auto brightness.

207

208 Images were integrated using R and the “tiff” package. Images were further processed
209 using GIMP 2.10. ImageJ and the MRI_wound_Healing_Tool.ijm macro plugin **[25]** were
210 used to process the images and calculate the area of the wound the cells have not
211 covered. Relative wound closure over time using time 0 for each condition as the control
212 was plotted and a curve line equation was formed by fitting the curve to a non-linear fit
213 one phase decay least squares fit with Yo=0 as a constraint. This base equation (Y=(Y0
214 - Plateau)*exp(-K*X) + Plateau) where Y0 is the Y value when X (time) is zero, Plateau is
215 the Y value at infinite times, and K is the rate constant, was used to determine the value
216 of X or half the time it takes to close the wound. Data were analyzed using GraphPad
217 Prism 9.

218

219 **Drug Resistance Screening**

220 Cells were seeded in 96-well plates at 2000 cells/well. Seeded cells were treated with a
221 range of gemcitabine concentrations. Cells were treated again 48 hours later. The number
222 of viable cells surviving drug treatment were measured with CellTiter-Glo (Promega
223 #G7571) 24 hours after the last drug treatment per the manufacturer's protocol using a
224 BioTek Synergy H5 plate reader. Sample size ranged from 4-11.

225

226 **Pathway Analysis**

227 1198 DEG from the ANGPTL4 OE vs KD analysis were imported into the KEGG Mapper-
228 Color **[26]** and Panther GO Enrichment Analysis **[27]**. The following parameters were
229 used for KEGG: Search mode: hsa, used uncolored diagrams, included aliases. The

following parameters were used for PANTHER: overrepresentation test, homo sapiens reference list, GO biological process complete, Fisher's exact test, and calculate FDR. Top pathways were merged manually and drawn using BioRender.

Overall Survival Analysis (OS)

To conduct survival analysis, clinical and RNA-seq expression data was retrieved from The Cancer Genome Atlas for 178 PDAC (TCGA-PAAD) patients (https://portal.gdc.cancer.gov/). Data were normalized using the R package DESeq2 and differentially expressed genes with an FDR < 0.1 were used to generate Kaplan-Meier survival curves. We classified tissues based on their average expression of a given gene set (bottom 25%, middle 50%, and top 25% of gene expression). We compared the patients with the lowest and highest quartile of average gene expression and performed survival analysis. Survival curves and analyses were generated using the "ggplot2", "survminer", and "survival" R packages. P values were generated using a log rank test.

Recurrence Free Survival (RFS)

A Kaplan Meier curve of recurrence-free survival survival plots for ANGPTL4 was created using GEPIA (http://gepia.cancer-pku.cn/) single gene analysis. The relevant parameters were as follows: Disease-free Survival (RFS), Group Cutoff: Quartile (75% high, 25% low), Hazards Ratio: Yes, 95% Confidence Interval: Yes, Axis Units: Months, and datasets Selection: PAAD.

Correlation Analysis

To compute correlation matrices, RNA-seq expression data was retrieved from The Cancer Genome Atlas for 178 PDAC (TCGA-PAAD) patients (https://portal.gdc.cancer.gov/).

Rank-based correlation coefficients were computed for each of the DEG with $\log_2$ fold change greater than 0.7 and baseMean>10 (MP2_ANGPTL4_KD vs MP2_ANGPTL4_OE with or without treatment) for 1) all TCGA-PAAD data DEG per gene vs ANGPTL4 expression and 2) all TCGA-PAAD data DEG gene versus OS time. These correlation values were used to generate a list of genes that are co-expressed with ANGPTL4 is overexpressed.

Correlation coefficients and p-values were computed using the "Hmisc" (version 4.6-0) R package. We classified tissues based on their ANGPTL4 expression of a given gene set (bottom 25%, middle 50%, and top 25% of gene expression). We computed correlation matrices using the expression data for patients with the lowest and highest quartile of ANGPTL4 expression which was used to divide samples into quantiles with highest and lowest average gene expression; based on expression of these 42 genes. (40 genes were measured in TCGA: KDM7a and STN1 were omitted).

Statistical Analysis

Statistical analysis was conducted in R (version 3.6.1 and R version 4.1.2 for RNAseq analysis). The following R packages and software were used for analysis:

survival (version 1.2.1335) **[28]**

276 survminer (version 0.4.9) **[29]**

277 ggplot2 (version 3.3.6) **[30]**

278 DESeq2 (version 1.24.0) **[31]**

279 pheatmap (version 1.0.12) **[32]**

280 Hmisc" (version 4.6-0) **[33]**

281 tiff (version 0.1-11) **[34]**

282

283

284 **RESULTS**

285 ***ANGPTL4* overexpression increases gemcitabine resistance genes in PDAC**

286 We previously showed that increased *ANGPTL4* expression in tumors is associated with

287 poor survival in PDAC patients (n=51) **[8]**. Here, we confirm the association with survival

288 in an independent cohort of 178 PDAC patients from The Cancer Genome Atlas (TCGA,

289 PAAD expression dataset). Patients with the highest (top 25%) expression of *ANGPTL4*

290 in tumor tissue had reduced overall survival (OS) and disease-free survival, (p=0.043 and

291 p=0.059 (log-rank test) (**Fig. 1A**, **Supplementary Fig. S1A)**.

292

293 Our previous findings motivated the current study to understand possible mechanisms by

294 which ANGPTL4 contributes to patient survival and specifically how it alters survival

295 outcomes through a possible role in drug resistance. We measured the impact of

296 *ANGPTL4* overexpression and knockdown in the MIA PaCa-2 cell line using CRISPRa

297 (MP2_ANGPTL4_OE) **[21]** and siRNA knockdown (MP2_ANGPTL4_KD). qPCR showed

298 CRISPRa successfully increased expression of the ANGPTL4 transcript by 8-fold

compared to a non-targeting control guide. Similarly, siRNA knockdown reduced expression by over 90% of the control line (**Fig. 1B, Supplementary Table S1**). An ELISA assay showed that protein levels were affected similarly (**Supplementary Fig. S1B**). We measured global gene expression changes using RNA-sequencing on the modified cell lines and controls which revealed 1198 differentially expressed genes (DEG) with a mean read count greater than 10, absolute $\log_2$Fold Change (log2FC) of at least 0.7, and adjusted p-value (padj) less than 0.05) when comparing overexpressed (OE) ANGPTL4 cells with the knockdown (KD) ANGPTL4 cells (**Supplementary Fig. S1C, Supplementary Table S2**). Given the observed association with drug resistance, we asked whether these DEGs were also associated with gemcitabine resistance by overlapping the 1198 DEG with 114 known gemcitabine resistance genes (**Supplementary Table S3**) **[35, 36, 37, 38]**. This revealed 15 gemcitabine resistance genes that are altered with overexpression of *ANGPTL4*, 10 of which overlap genes that are part of the EMTome (**Fig. 1C) [39].** Several of these genes are linked to activation of TGF**β** and its downstream signaling pathways: ERK, PI3K/AKT, and JNK (SH3RF2, TGFBR3, PPP1R15A, INPP4B, WWTR1, and FGF2), contributors to EMT (SOX9, CUL7, and TGFBR3), and transcriptional regulation of pluripotent stem cells (STAT3, KLF4, and FGF2) **[26, 27]**. Additional pathway analysis showed a connection between the expression of ANGPTL4 and EMT (GO:0001837) in the presence (3.24-fold enrichment, 0.0273 FDR) or absence (3.04-fold enrichment, 0.195 FDR) of gemcitabine treatment (**Supplementary Table S4-S5**).

Figure 1

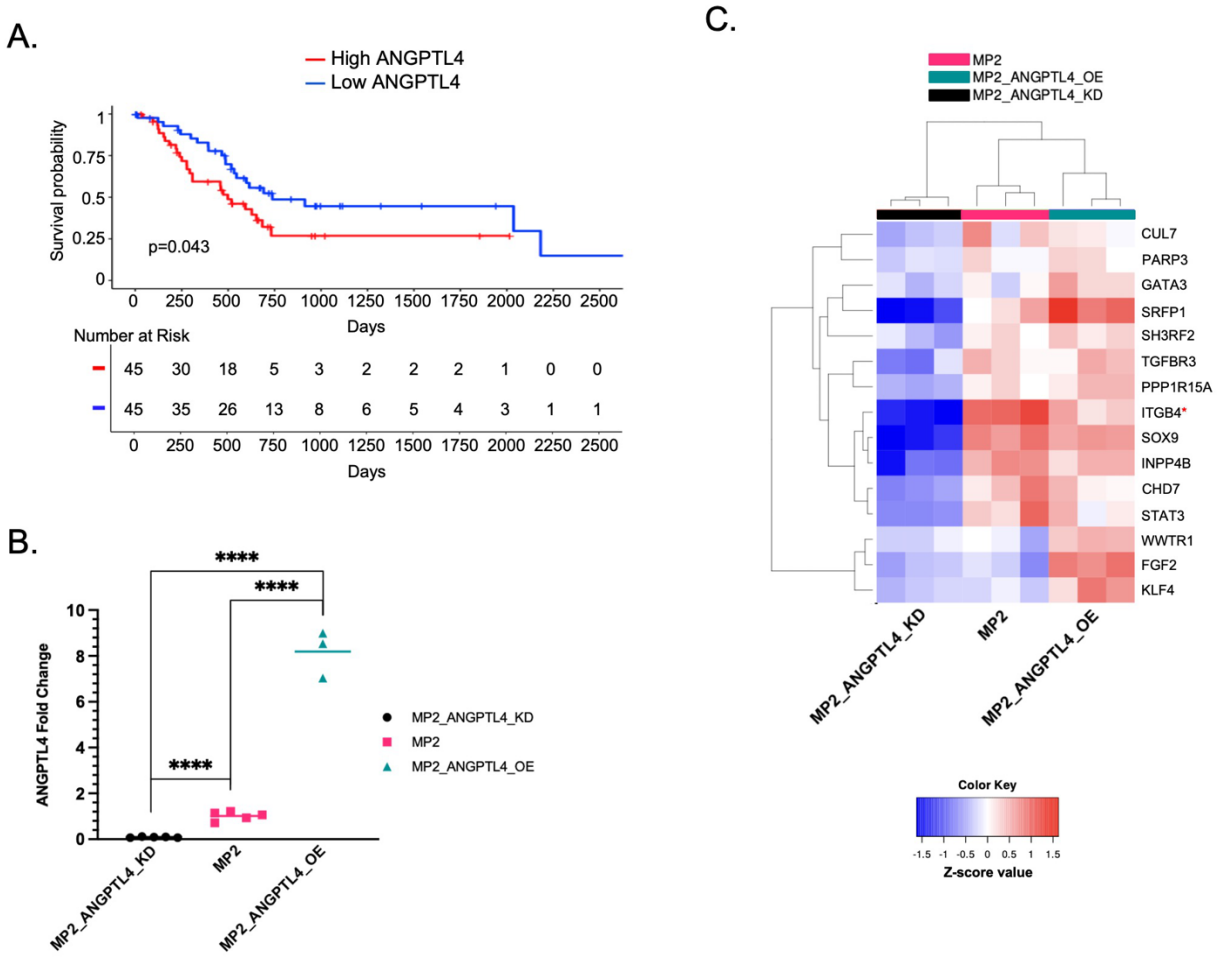

Figure 1: Expression of *ANGPTL4* is associated with patient outcomes and modifies expression of resistance-associated genes.

a) A Kaplan Meier curve for overall survival using TCGA-PAAD data. The patients with the top (red) and bottom (blue) 25% average *ANGPTL4* gene expression have significantly different OS. (p=0.043, log-rank test) **b)** Relative expression of ANGPTL4 transcript in MP2_ANGPTL4_KD (black circles), MP2 (pink squares), and MP2_ANGPTL4_OE (turquoise triangles) as measured by qPCR. P-values from unpaired, two-tailed parametric t-tests performed with 95% confidence intervals are displayed. Values are normalized with *ACTB* as the housekeeper. (P-values ≤

331 0.0001=****) **c)** Heatmap displaying RNA-seq results from MP2_ANGPTL4_KD (black),

332 MP2_NTC (pink), and MP2_ANGPTL4_OE (turquoise) cell lines. Displayed are 15 genes
333 associated with both ANGPTL4 overexpression and gemcitabine resistance. Normalized
334 expression for each of the 15 genes is plotted in the heatmap. Red (*) indicates ITGB4
335 used for later experiments.

336

337 **Increased *ANGPTL4* expression alters cellular response to gemcitabine**

338 We assessed whether altering *ANGPTL4* expression impacted response to gemcitabine
339 to explore the potential impact of *ANGPTl4* overexpression on treatment response in
340 patients. We measured cell viability in MP2_ANGPTL4_KD and MP2_ANGPTL4_OE cell
341 lines before and after treatment with gemcitabine. As expected, treatment with 12.5nM
342 gemcitabine reduces viability compared to untreated cells. Comparing cells with
343 overexpression of *ANGPTL4* to controls, we observed an increase in cell viability with the
344 same gemcitabine concentrations. Similarly, there was a significant reduction in viability
345 with the *ANGPTL4* knockdown compared to cells overexpressing *ANGPTL4*. This
346 difference in viability is not observed in the untreated cells **(Fig. 2A, Supplementary**
347 **Table S1)**. These results demonstrate a greater sensitivity to gemcitabine with reduction
348 of ANGPTL4. To understand the link between ANGPTL4 expression and gemcitabine
349 response, we measured transcriptional response to gemcitabine in MP2_ANGPTL4_OE
350 cells and MP2_ANGPTL4_KD cells using RNA-sequencing. We were not surprised to
351 note that 955 genes were differentially expressed upon treatment with the cytotoxic
352 gemcitabine alone. We explored the intersection of the 1198 DEGs identified upon
353 *ANGPTL4* overexpression and the 955 DEGs associated with gemcitabine treatment.

354 This analysis revealed 42 genes associated with gemcitabine response and *ANGPTL4*
355 overexpression (**Fig. 2B, Supplementary Table S6).** This strategy nominated genes that
356 might contribute to altered response to gemcitabine in cells overexpressing *ANGPTL4*
357 and are potentially important for patient outcomes. We tested whether these genes were
358 predictive of patient overall survival using data from TCGA. Since all 42 transcripts were
359 positively correlated with ANGPTL4 expression, we calculated the mean gene expression
360 of these genes and found that patients whose tumors had the highest average expression
361 had significantly reduced overall survival (p=0.0073, **Figure 2C**). The fraction of patients
362 surviving 1500 days or more is dramatically increased in the individuals with low
363 expression of these 42 ANGPTL4 and gemcitabine response genes. This compares
364 favorably to the average 3-year relative survival for PDAC patients in the United States
365 with resectable stage I/II disease- 17% **[40]**.

Figure 2

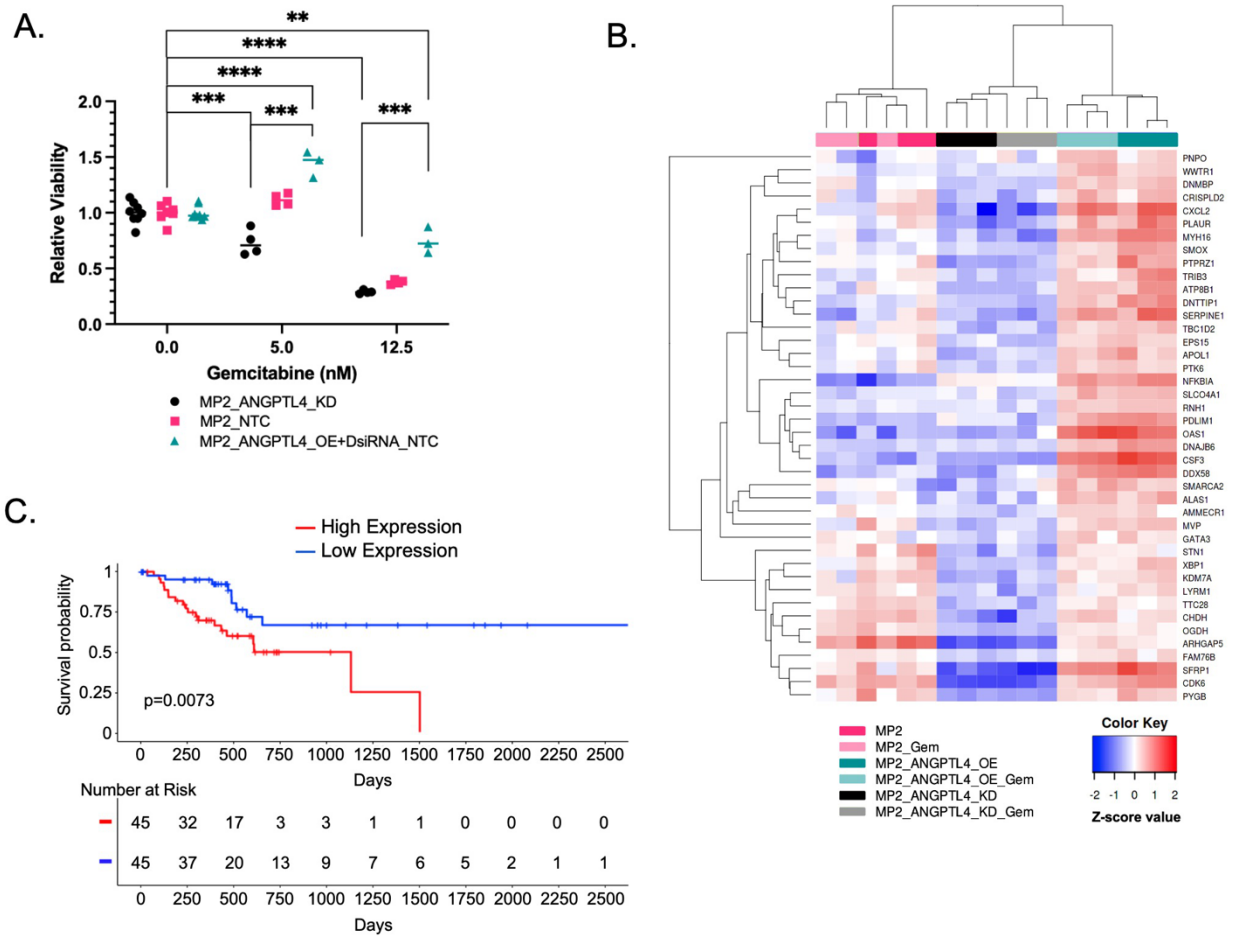

Figure 2: Gemcitabine resistance signature in PDAC cells with high ANGPTL4

a) Cell viability was measured for MP2_ANGPTL4_KD (black), MP2_NTC (pink), and MP2_ANGPTL4_OE (turquoise) cells treated with 0, 5nM, or 12.5nM gemcitabine. Relative viability reflects normalization to cells not treated with gemcitabine. P-value asterisks: ≤0.01=**, ≤0.001=*** & ≤0.0001=****, unpaired, two-tailed t-test **b)** Heatmap of gene expression measured by RNA-seq in MP2_ANGPTL4_KD (black/gray), MP2 (pink/light pink), and MP2_ANGPTL4_OE (turquoise/aqua) cell lines both untreated and treated with 1.5nM gemcitabine. Normalized expression of the 42 genes that resulted

375 from an intersection of ANGPTL4 expression DEGs and gemcitabine treatment response
376 DEGs are included in the heatmap. **c)** Kaplan-Meier curve for overall survival using
377 TCGA-PAAD data where patients were divided into quartiles with highest (red) and lowest
378 (blue) using mean expression of the 42 genes in the intersection (40 genes were available
379 in TCGA: *KDM7a* and *STN1* were omitted). P-values were derived from a log-rank test.
380

381 ***ITGB4* and *APOL1* inhibition sensitizes high *ANGPTL4* cells to gemcitabine**

382 I*n vitro* overexpression of *ANGPTL4* alters cellular drug response and correlates with
383 patient survival but the pathway(s) by which this resistance is achieved are unknown. We
384 reasoned that genes co-regulated with ANGPTL4 may function with ANGPTL4 and
385 contribute to resistance and found those genes by identifying genes that are co-
386 expressed with *ANGPTL4* in patient tissues. For each of the 1198 DEGs identified when
387 *ANGPTL4* was overexpressed *in vitro*, we calculated rank-based correlation coefficients
388 and identified co-expressed genes in patient tissues (TCGA-PAAD). For each gene with
389 a significant correlation with ANGPTL4 in patient tissues, we determined whether
390 expression of that gene alone was significantly correlated with patient overall survival
391 (**Supplementary Table S7**). This allowed further filtering of the list based on the
392 assumption that true resistance-associated genes would impact patient survival. From
393 this list, ITGB4 and APOL1 are both positively correlated with *ANGPTL4* expression *in*
394 *vitro* and in patients, altered with gemcitabine response *in vitro*, and correlated with
395 patient survival in tissues. While there are several genes of interest, we focused on ITGB4
396 and APOL1 in this study, in part based on their drugability (pharos.nih.gov) and availability
397 of efficient siRNA knockdown reagents. Based on the co-expression with ANGPTL4 and

398 the link to patient survival, we tested whether expression of these genes in combination
399 with ANGPTL4 was relevant for patient outcomes. Comparing tissues that were among
400 the top 25% expression of both *ANGPTL4* and *APOL1* (**Fig. 3A**) or ITGB4 (**Fig. 3B**) to
401 those that were among the bottom 25% expression of both *ANGPTL4* and *APOL1* or
402 *ITGB4* we saw significant differences in overall survival, with overall survival being worse
403 for TCGA-PAAD patients with high ANGPTL4 combined with high APOL1 (p = 0.014) or
404 ITGB4 (p = 0.01) expression. Tumors with high levels (top 25%) of all three genes;
405 *APOL1*, *ITGB4*, and *ANGPTL4,* also had reduced survival compared with the bottom
406 25%, but when APOL1 and ITGB4 are combined with ANGPTL4 expression the reduction in
407 survival did not become more significant (p = 0.015) (**Supplementary Fig. S1D).**
408
409 Given the association of ANGPTL4 with resistance and patient outcome, we tested
410 whether, like ANGPTL4, loss of *ITGB4* or *APOL1* expression increased sensitivity to
411 gemcitabine *in vitro*. Using siRNAs, we knocked down *APOL1* and *ITGB4* in the
412 MP2_ANGPTL4_OE cell line. We showed that treatment with the siRNAs reduced mRNA
413 levels of the target genes (**Supplementary Figure S2A-B**), and we also found that
414 knockdown of *ITGB4* or *APOL1* reduced expression of *ANGPTL4* significantly compared
415 to a non-targeting siRNA control with ANGPTL4 overexpression background; expression
416 was reduced to 2% in MP2, 5% in ITGB4 knockdown, and 25% in APOL1 knockdown
417 **(Fig. 3C, Supplementary Table S1).** Given our previous finding that overexpression of
418 *ANGPTL4* leads to resistance, we hypothesized that knockdown of *APOL1* and *ITGB4*
419 might reverse resistance given the impact on *ANGPTL4* expression. We tested the impact
420 of *ITGB4* and *APOL1* knockout on gemcitabine sensitivity in the MP2_ANGPTL4_OE line.

421 After gemcitabine treatment, cells with knockdown of *ITGB4* or *APOL1* in the
422 ANGPTL4_OE background (MP2_ANGPTL4_OE_ITGB4_KD or
423 MP2_ANGPTL4_OE_APOL1_KD) showed reversal of drug resistance when compared
424 to the ANGPTL4 OE cells **(Fig. 3D).** There was no difference in growth rate among the
425 lines that explained the differential viability observed with gemcitabine treatment
426 **(Supplementary Fig. S2C).**

Figure 3

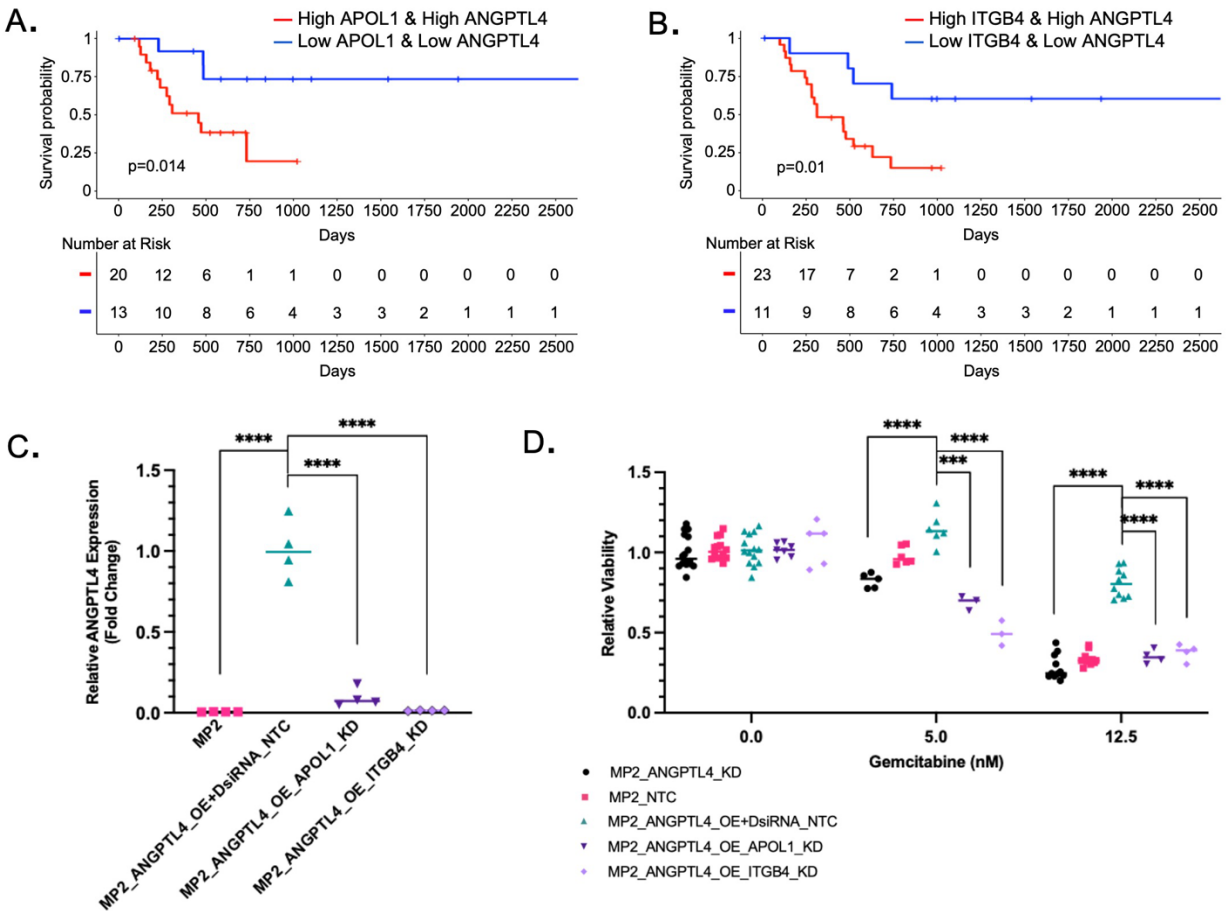

427

428 **Figure 3: ITGB4 and APOL1 inhibition sensitizes cells overexpressing ANGPTL4 to**
429 **gemcitabine.**

430 **a-b)** Kaplan-Meier plot for overall survival using TCGA-PAAD data. Patients with the top
431 (red) and bottom (blue) 25% average ANGPTL4 gene expression and APOL1 or ITGB4
432 gene expression (p=0.01 and p=0.014, respectively, log-rank test). **c)** ANGPTL4
433 expression measured by qPCR normalized to MP2_ANGPTL4_OE+DsiRNA_NTC
434 (turquoise) control: MP2 (pink), MP2_ANGPTL4_OE_ITGB4_KD (lavender), and
435 MP2_ANGPTL4_OE_APOL1_KD (purple) compared to mean of
436 MP2_ANGPTL4_OE+DsiRNA_NTC (MP2_ANGPTL4_OE cells transduced with non-
437 targeting control siRNA). Expression is normalized to the housekeeping gene ACTB. P-
438 values ≤ 0.0001=****; unpaired two-tailed parametric t-test **d)** Relative viability is plotted
439 by normalizing all data to cells not treated with gemcitabine. MP2_ANGPTL4_KD (black),
440 MP2_NTC (pink), MP2_ANGPTL4_OE+DsiRNA_NTC (turquoise),
441 MP2_ANGPTL4_OE_ITGB4_KD (lavender), and MP2_ANGPTL4_OE_APOL1_KD
442 (purple) cells treated with 0, 5nM, or 12.5nM gemcitabine. Sample size ranges from 4-
443 11 per condition. P-value asterisks: ≤0.001=*** & ≤0.0001=****, unpaired, two-tailed
444 parametric t-tests.
445

446 ***ANGPTL4* overexpression increases cell migration**

447 To further understand the pathways that might be involved in resistance, we performed
448 pathway enrichment analysis on the 1198 DEG associated with overexpression of
449 *ANGPTL4* (OE v KD). Those included tumor invasion and metastasis, proliferation,
450 differentiation, inhibition of apoptosis, and cell membrane formation. Genes participating
451 in invasion and metastasis included RhoEGF which was increased with *ANGPTL4*
452 expression. RhoEGF is linked to tumor invasion and metastasis **[41]**. Many genes in the

453 Ras-ARF6 and Ras-MEK2 signaling pathways are also upregulated (e.g. *FGF, APOL1,*
454 *ITGB4, EGFR, MPK, CREB, cFOS, JUN*, and *VEGF*) impacting proliferation and
455 differentiation. In addition, ANTPGL4 overexpression is associated with the upregulation
456 of anti-apoptotic pathways including JAK-STAT, Bcl_XS, and SOCS pathways triggered
457 by upregulation of cytokine, cytokine receptors, *CNTF*, and *IL22RA2*. The formation of
458 cellular structure was also affected by *ANGPTL4* and increase in Claudin via the decrease
459 in cell permeability (*GEF-H1, Claudin2*), increased actin assembly (*ARP2/3*), and cell
460 polarity (*AMPK, DLG1*) (**Fig. 4A, Supplementary Table S8).**
461
462 Others have shown that on their own *ANGPTL4, APOL1,* and *ITGB4* are each associated
463 with cell proliferation and contribute to PDAC progression **[17, 42, 43]**. We measured
464 migration using a wound healing time course assay to determine if the increased
465 migration associated with *ANGPTL4* overexpression could be reversed with the KD of
466 *ITGB4* or *APOL1* (**Fig. 4B).** We observed that knockdown of either *APOL1* or *ITGB4* in
467 lines overexpressing *ANGPTL4* reduced the migratory potential of these cells. This was
468 apparent 48 hours after the scratch was made and was quantified by calculating the time
469 to close half of the gap (t1/2 gap) for each of the four cell types is plotted. (**Fig. 4C,**
470 **Supplementary Table S1).**

Figure 4

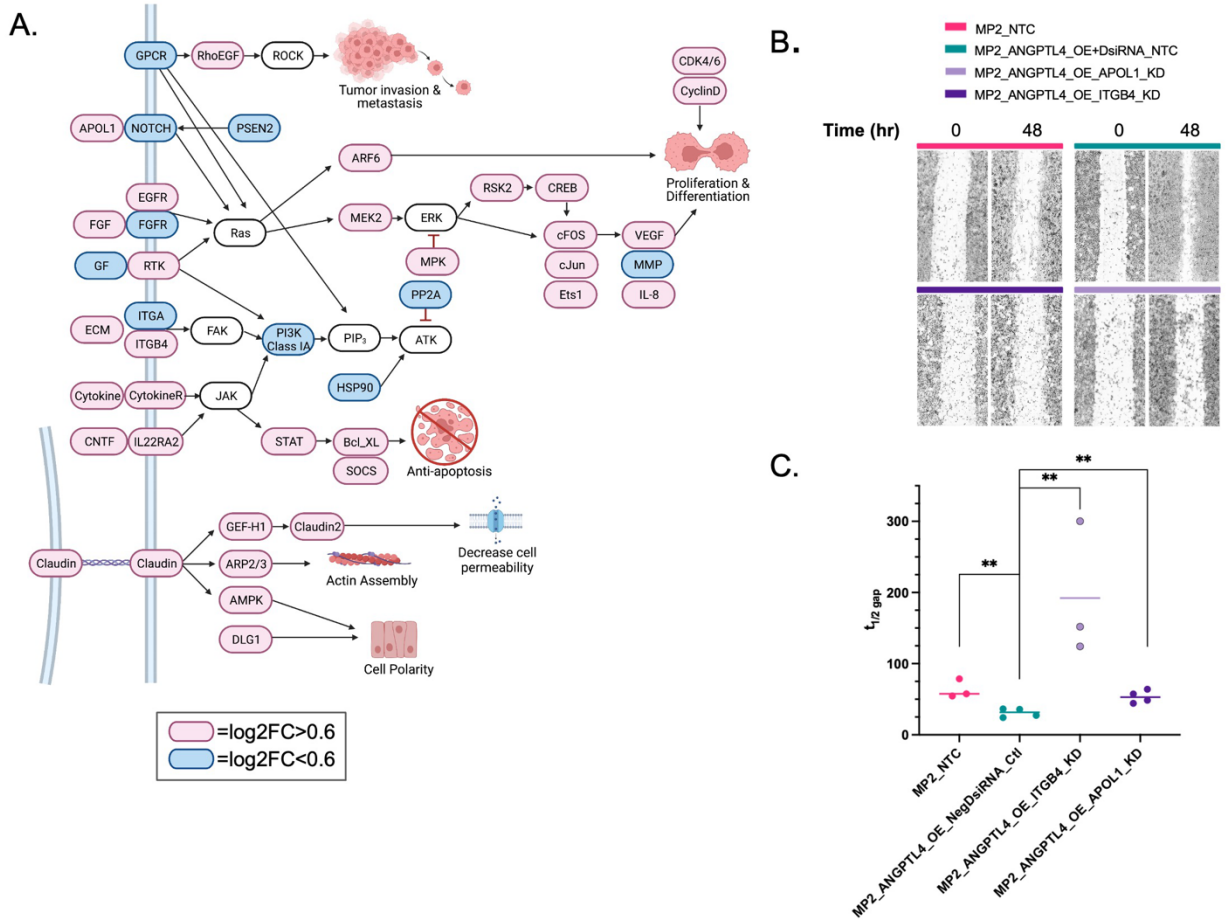

Figure 4: ANGPTL4 overexpression correlation with EMT.

a) Pathway analysis of 1198 DEG revealed common cancer pathways. Red=$\log_2$FC >0.7 and Blue=$\log_2$FC <0.7. **b)** Wound healing assay results at 0 hrs (after initial wound) and 48 hours MP2_NTC (pink), MP2_ANGPTL4_OE+DsiRNA_NTC (turquoise), MP2_ANGPTL4_OE_ITGB4_KD (lavender), and MP2_ANGPTL4_OE_APOL1_KD (purple). Each set was performed in triplicate or quadruplicate. **c)** Time to close half the gap (t1/2 gap) for each of the four cell types is plotted. t1/2: MP2=57.7hrs, MP2_ANGPTL4_OE= 31.6 hrs., MP2_ANGPTL4_OE_ITGB4_KD= 192 hrs., and MP2_ANGPTL4_OE_APOL1_KD=52.96 hrs. P-values ≤0.01=**, unpaired parametric t-

481 test.

482

483

484 **DISCUSSION**

485 Here we have described how overexpression of *ANGPTL4* in pancreatic cancer
486 contributes to disease progression and resistance. We have shown that overexpression
487 of this gene and protein leads to cellular resistance to gemcitabine, one of the most
488 commonly used chemotherapeutics in PDAC. It follows that if overexpression leads to
489 chemoresistance, increased expression of this gene would also be associated with poor
490 patient outcomes, and we confirmed that in independent patient cohorts. The goal of our
491 study is to further understand the role of this gene in chemoresistance in the hopes that
492 a mechanistic understanding will facilitate the development of new treatment strategies.
493 Our transcriptomic analysis revealed that overexpression of *ANGPTL4* broadly impacts
494 transcriptomic profiles in pancreatic cancer cells. This is perhaps not surprising given a
495 rather large body of literature describing not only ANGPTL4's role in cancer but also
496 cardiovascular disease risk and metabolism **[9]**. In fact, ANGPTL4's role in cancer can
497 be difficult to summarize because it has been shown to have both protective and
498 promoting effects in different cancer types **[13]**. Our initial findings highlighted the
499 potential importance of this gene and existing literature was not sufficient to understand
500 how this gene functions in pancreatic cancer. Using our transcriptomic data, we narrowed
501 our analysis to a list of *ANGPTL4*-impacted genes that are also responsive to gemcitabine
502 treatment *in vitro*. We identified 42 genes associated with *ANGPTL4* overexpression and

503 gemcitabine response and determined that the expression of those genes effectively
504 predicted patient outcomes.
505
506 Further narrowing our focus, we identified *APOL1* and *ITGB4* among the genes that are
507 associated with *ANGPTL4* overexpression, gemcitabine resistance, and patient survival
508 and explored them further. We found that knockdown of either *APOL1* or *ITGB4* increased
509 sensitivity to gemcitabine in cells overexpressing *ANGPTL4*. This finding confirms that
510 inhibition of *APOL1* or *ITGB4* can reverse resistance associated with *ANGPTL4*
511 expression in pancreatic cancer cells. One unexpected finding was that knockdown of
512 these genes also reduced expression of *ANGPTL4* itself. Rather than our initial
513 hypothesis that expression of *ANGPTL4* was correlated with *APOL1* or *ITGB4* because
514 they were regulated by *ANGPTL4*, this data supports the hypothesis that *ANGPTL4* is
515 regulated, directly or indirectly, by *APOL1* and *ITGB4* and these genes could be involved
516 in a feedback loop that explains our results.
517
518 Considering *APOL1* first, APOL1 (apolipoprotein L1) is part of the HDL lipid complex
519 which plays a key role in lipid metabolism **[44]**. APOL1 can activate NOTCH1 signaling
520 leading to reduced proliferation and increased apoptosis **[42]**. NOTCH1 also upregulates
521 ABCC1, a transporter that can also lead to multidrug resistance **[45]**. In other contexts,
522 NOTCH1 also has been shown to stabilize and activate PPARγ, a transcription factor that
523 promotes transcription of ANGPTL4 **[46]**. These results suggest a possible mechanism
524 by which knockdown of *APOL1* may reduce *ANGPTL4* expression and further suggests
525 that inhibition of *APOL1*, especially in patients with high expression of *ANGPTL4* might

526 reduce cellular capacity for migration and proliferation. Additional studies would need to
527 be performed to demonstrate whether the link between ANGPTL4 and APOL1 requires
528 NOTCH signaling.
529
530 *ITGB4* knockdown also reduces *ANGPTL4* overexpression. ITGB4 (integrin β4, α6β4) is
531 an integrin protein that plays a role in cell-extracellular matrix adhesion. It is upregulated
532 in several cancers including pancreatic cancer and has been linked to poor prognosis,
533 high tumor grade, lymph node metastasis, and drug response [**47, 48, 49]**. Knockdown
534 of *ITGB4* increases cisplatin sensitivity in lung cancer models **[47]** suggesting that *ITGB4*
535 is relevant for resistance to multiple chemotherapeutics. ITGB4 may promote receptor
536 tyrosine kinase (RTK) activation through ERBB2 **[50]**. RTKs generally promote
537 proliferation, invasion, and sustained cell migration, and ITGB4 has a synergistic effect in
538 combination with increased RTKs expression **[50, 51]**. In our study, we observed
539 increased expression of *CSF3, VEGFA, HBEGF,* and *DDR2*, which all play a role in the
540 epithelial-to-mesenchymal transition in cells overexpressing *ANGPTL4*. An alternate
541 hypothesis is that *ITGB4* promotes cell migration and invasion through regulation of the
542 MEK1-ERK1/2 signaling cascade **[49]**. Reduction of *ITGB4* in the context of
543 overexpressed *ANGPTL4* could also affect this pathway, explaining the reduced
544 migratory potential of *ITGB4* KD cells in the cells overexpressing *ANGPTL4*. Additional
545 transcriptomic and biochemical studies are needed to determine which of these pathways
546 are most relevant for the chemoresistance phenotypes.
547
548

549 **CONCLUSIONS**

550 Our study provides evidence that *ANGPTL4* overexpression in pancreatic cancer impacts
551 several key signaling and metabolic pathways associated with patient survival, in part
552 through controlling cellular resistance to chemotherapy and cellular migration. *ITGB4* and
553 *APOL1* knockdown are both able to reverse drug resistance and migration increases
554 associated with overexpression of *ANGPTL4* but appear to do so through different
555 mechanisms. These findings emphasize the complexity of developing treatments to target
556 resistance and metastasis; a single approach may not be sufficient. Nonetheless, both
557 *APOL1* and *ITGB4* represent potential novel targets and our data support the further
558 exploration of these genes and the pathways in which they function.

559

560

561 **ABBREVIATIONS**

562 ***AKT:*** AKT Serine/Threonine Kinase 1

563 ***AMPK:*** Protein Kinase AMP-Activated Catalytic Subunit Alpha 1

564 ***ANGPTL4:*** Angiopoietin Like 4

565 ***ARP2/3:*** Actin Related Protein 2/3

566 ***APOL1:*** Apolipoprotein L1

567 ***Bcl_XS:*** BCL2 Apoptosis Regulator

568 ***cFOS:*** Fos Proto-Oncogene, AP-1 Transcription Factor Subunit

569 ***CNTF:*** Ciliary Neurotrophic Factor

570 ***CO_2:*** carbon dioxide

571 ***CREB:*** CAMP Responsive Element Binding Protein

572 ***CRISPRa:*** dCas9 activation system

573 ***CSF3:*** colony-stimulating factor 3

574 ***CUL7:*** Cullin 7

575 ***DAVID:*** Database for Annotation, Visualization, and Integrated Discovery

576 ***DEG:*** differentially expressed genes

577 ***DDR2:*** Discoidin Domain Receptor Tyrosine Kinase 2

578 ***DLG1:*** Discs Large MAGUK Scaffold Protein 1

579 ***DsiRNA:*** Dicer-substrate small interfering RNA

580 ***EMT:*** epithelial to mesenchymal transition

581 ***EGFR:*** Epidermal Growth Factor Receptor

582 ***ERK:*** Mitogen-Activated Protein Kinase 1

583 ***ERK1/2:*** Mitogen-Activated Protein Kinase 1/2

584 ***FGF:*** Fibroblast Growth Factor 1

585 ***FGF2***: Fibroblast Growth Factor Receptor 2

586 ***FOS:*** Fos Proto-Oncogene, AP-1 Transcription Factor Subunit

587 ***GEO:*** Gene Expression Omnibus

588 ***GEPIA:*** Gene Expression Profiling Interactive Analysis

589 ***GEF-H1:*** Rho/Rac Guanine Nucleotide Exchange Factor 2

590 ***HBEGF:*** Heparin Binding EGF-Like Growth Factor

591 ***INPP4B:*** Inositol Polyphosphate-4-Phosphatase Type II B

592 ***ITGB4:*** Integrin Subunit Beta 4

593 ***JAK:***Janus Kinase 1

594 ***JNK:*** Mitogen-Activated Protein Kinase 8

595 ***JUN:*** Jun Proto-Oncogene, AP-1 Transcription Factor Subunit

596 ***KD:*** knockdown

597 ***KEGG:*** Kyoto Encyclopedia of Genes and Genomes

598 ***KDM7a:*** Lysine Demethylase 7A

599 ***KLF4:*** KLF Transcription Factor 4

600 ***KRAS:*** KRAS Proto-Oncogene, GTPase

601 ***IL22RA2:*** Interleukin 22 Receptor Subunit Alpha 2

602 ***MEK1:*** Mitogen-Activated Protein Kinase

603 ***MP2:*** MIA PaCa-2 cells

604 ***MPK:*** Mitogen-Activated Protein Kinase

605 ***n:*** number

606 ***ng:*** nanograms

607 ***nM:*** nanomolar

608 ***NOTCH:*** Notch Receptor

609 ***OE:*** overexpression

610 ***OS:*** overall survival

611 ***p:***p-value

612 ***PAAD:*** pancreatic ductal adenocarcinoma

613 ***padj:*** adjusted p-value

614 ***PARP:*** Poly(ADP-Ribose) Polymerase

615 ***PDAC:*** pancreatic ductal adenocarcinoma

616 ***PI3K:*** Phosphatidylinositol-4,5-Bisphosphate 3-Kinase Catalytic Subunit Delta

617 ***PPP1R15A:*** Protein Phosphatase 1 Regulatory Subunit 15A

618 ***qPCR:*** quantitative polymerase chain reaction

619 ***RFS:*** recurrence-free survival

620 ***SEER:*** Surveillance, Epidemiology, and End Results

621 ***SH3RF2:*** SH3 Domain Containing Ring Finger 2

622 ***siRNA:*** silencing RNA

623 ***SOCS:*** Suppressor of Cytokine Signaling

624 ***SOX9:*** SRY-Box Transcription Factor 9

625 ***STAT:*** Signal Transducer and Activator of Transcription 3

626 ***STAT3:*** Signal Transducer and Activator of Transcription 3

627 ***STN1:*** STN1 subunit of CTS complex

628 ***TCGA:*** The Cancer Genome Atlas

629 ***TGFβ:*** TGFB Induced Factor Homeobox 1

630 ***TGFBR3:*** Transforming Growth Factor Beta Receptor 3

631 ***uL:*** microliter

632 ***v:*** versus

633 ***VEGF:*** Vascular Endothelial Growth Factor A

634 ***VEGFA:*** Vascular Endothelial Growth Factor A

635 ***WWTR1:*** WW Domain Containing Transcription Regulator 1

636

637

638 **DECLARATIONS**

639 **Consent for Publication**

640 NA

641

642 **Data Availability**

643 The RNA-seq data generated in this study are available in Gene Expression Omnibus
644 (GEO) at GSE207359. Clinical data and RNA-sequencing data for TCGA-PAAD
645 (PDAC) samples were retrieved on 04/01/2020 using the GDC Data Portal
646 (https://portal.gdc.cancer.gov/projects/TCGA-PAAD). Our analyses included 178 samples
647 in this cohort that had matched clinical and RNA sequencing data.

648

649 **Competing interests**

650 The authors declare that they have no competing interests.

651

652 **Funding**

653 This work was funded by NIH 1R43CA232844-01A1 and the State of Alabama Cancer
654 Research Fund.

655

656 **Authors' contributions**

657 ERG, CAW, and SJC designed the experiments. ERG, CAW, and MJ collected data. ERG
658 and CAW analyzed the data. ERG and SJC wrote the first draft. All authors contributed
659 to the writing of the paper and read and approved the final manuscript.

660

661 **Acknowledgements**

662 This work was funded by NIH 1R43CA232844-01A1 and the State of Alabama Cancer
663 Research Fund. SJC is supported by UL1TR003096. We would like to thank Anuj Singhal

and his team at CFD Research as well as our HudsonAlpha colleagues, especially those in the Myers lab for their feedback, support, and discussions of this work. Figure 4A created with BioRender.com agreement number RD24SQPZ3K.

Ethics Declaration

All methods were carried out in accordance with relevant guidelines and regulations.

REFERENCES

1. U.S. Mortality Data 1969-2019 when Using SEER*Stat: Surveillance, Epidemiology, and End Results (SEER) Program (www.seer.cancer.gov) SEER*Stat Database: Mortality - All COD, Aggregated With State, Total U.S. (1969-2019) [Internet]. 2021. Available from: http://www.cdc.gov/nchs
2. Sturm N, Ettrich TJ, Perkhofer L. The Impact of Biomarkers in Pancreatic Ductal Adenocarcinoma on Diagnosis, Surveillance and Therapy. *Cancers* 2022;14(1)217. http://dx.doi.org/10.3390/cancers14010217
3. Conroy T, Desseigne F, Ychou M, Bouché O, Guimbaud R, Bécouarn Y, Adenis A, Raoul JL, Gourgou-Bourgade S, de la Fouchardière C, Bennouna J, Bachet JB, Khemissa-Akouz F, Péré-Vergé D, Delbaldo C, Assenat E, Chauffert B, Michel P, Montoto-Grillot C, Ducreux M; Groupe Tumeurs Digestives of Unicancer; PRODIGE Intergroup. FOLFIRINOX versus gemcitabine for metastatic pancreatic cancer. *N Engl J Med*. 2011;364(19):1817-25. doi: 10.1056/NEJMoa1011923. PMID: 21561347.

687 4. American Cancer Society. Cancer Facts & Figures 2022. Atlanta; 2022.
688 5. Javle M, Shacham-Shmueli E, Xiao L, Varadhachary G, Halpern N, Fogelman D,
689 et al. Olaparib Monotherapy for Previously Treated Pancreatic Cancer With DNA
690 Damage Repair Genetic Alterations Other Than Germline BRCA Variants: Findings
691 From 2 Phase 2 Nonrandomized Clinical Trials. *JAMA Oncology* 2021;7:693–9.
692 6. Moore MJ, Goldstein D, Hamm J, Figer A, Hecht JR, Gallinger S, et al. Erlotinib
693 plus gemcitabine compared with gemcitabine alone in patients with advanced
694 pancreatic cancer: A phase III trial of the National Cancer Institute of Canada
695 Clinical Trials Group. *J Clin Oncol. American Society of Clinical Oncology*
696 2007;25:1960–6.
697 7. Pishvaian MJ, Bender RJ, Halverson D, Rahib L, Hendifar AE, Mikhail S, et al.
698 Molecular profiling of patients with pancreatic cancer: Initial results from the know
699 your tumor initiative. Clin Cancer Res. *American Association for Cancer Research*
700 *Inc.* 2018;24:5018–27.
701 8. Kirby MK, Ramaker RC, Gertz J, Davis NS, Johnston BE, Oliver PG, et al. RNA
702 sequencing of pancreatic adenocarcinoma tumors yields novel expression patterns
703 associated with long-term survival and reveals a role for ANGPTL4. *Mol Oncol.*
704 2016;10:1169–82.
705 9. Fernández-Hernando C, Suárez Y. ANGPTL4: A multifunctional protein involved in
706 metabolism and vascular homeostasis. *Current Opinion in Hematology* 2020. page
707 206–13. Available from: http://dx.doi.org/10.1097/MOH.0000000000000580
708 10. La Paglia L, Listì A, Caruso S, Amodeo V, Passiglia F, Bazan V, et al. Potential
709 Role of ANGPTL4 in the Cross Talk between Metabolism and Cancer through

710 PPAR Signaling Pathway. *PPAR Research* 2017.
711 http://dx.doi.org/10.1155/2017/8187235
712 11. Lei X, Shi F, Basu D, Huq A, Routhier S, Day R, et al. Proteolytic processing of
713 angiopoietin-like protein 4 by proprotein convertases modulates its inhibitory effects
714 on lipoprotein lipase activity. *J Biol Chem. American Society for Biochemistry and*
715 *Molecular Biology Inc.* 2011;286:15747–56.
716 12. Kim SH, Park YY, Kim SW, Lee JS, Wang D, DuBois RN. ANGPTL4 induction by
717 prostaglandin E 2 under hypoxic conditions promotes colorectal cancer
718 progression. *Cancer Res.* 2011;71:7010–20.
719 13. Tan MJ, Teo Z, Sng MK, Zhu P, Tan NS. Emerging roles of angiopoietin-like 4 in
720 human cancer. *Molecular Cancer Research* 2012;10(6):677–88.
721 http://dx.doi.org/10.1158/1541-7786.MCR-11-0519
722 14. Zhu P, Tan MJ, Huang RL, Tan CK, Chong HC, Pal M, et al. Angiopoietin-like 4
723 Protein Elevates the Prosurvival Intracellular O2-:H2O2 Ratio and Confers Anoikis
724 Resistance to Tumors. Cancer Cell. *Cell Press* 2011;19:401–15.
725 15. Teo Z, Sng MK, Chan JSK, Lim MMK, Li Y, Li L, et al. Elevation of adenylate energy
726 charge by angiopoietin-like 4 enhances epithelial-mesenchymal transition by
727 inducing 14-3-3γ expression. *Oncogene* 2017;36:6408–19.
728 16. Zhang K, Zhai Z, Yu S, Tao Y. DNA methylation mediated down-regulation of
729 ANGPTL4 promotes colorectal cancer metastasis by activating the ERK pathway.
730 *J Cancer* 2021;12:5473–85.

731 17. Zhao J, Liu J, Wu N, Zhang H, Zhang S, Li L, et al. ANGPTL4 overexpression is
732 associated with progression and poor prognosis in breast cancer. *Oncol Lett*.
733 2020;20:2499–505.
734 18. Cai YC, Yang H, Wang KF, Chen TH, Jiang WQ, Shi YX. ANGPTL4 overexpression
735 inhibits tumor cell adhesion and migration and predicts favorable prognosis of triple-
736 negative breast cancer. *BMC Cancer* 2020;20. http://dx.doi.org/10.1186/s12885-
737 020-07343-w
738 19. Yan HH, Jung KH, Lee JE, Son MK, Fang Z, Park JH, et al. ANGPTL4 accelerates
739 KRASG12D-Induced acinar to ductal metaplasia and pancreatic carcinogenesis.
740 *Cancer Lett*. 2021;519:185–98.
741 20. Gupta N, Park JE, Tse W, Keem Low J, Kon OL, Mccarthy N, et al. ERO1α
742 promotes hypoxic tumor progression and is associated with poor prognosis in
743 pancreatic cancer. *Oncotarget* 2019;10(5):5870-5982.
744 https://www.oncotarget.com/article/27235/text/
745 21. Joung, J., Konermann, S., Gootenberg, J. S., Abudayyeh, O. O., Platt, R. J.,
746 Brigham, M. D., Sanjana, N. E., & Zhang, F. Genome-scale CRISPR-Cas9
747 knockout and transcriptional activation screening. *Nature Protocols*; 2017; *12*(4),
748 828–863. https://doi.org/10.1038/nprot.2017.016
749 22. Larson B, Held P, Banks P. Optimization of Perkin Elmer's AlphaScreen® cAMP
750 Assay on the Synergy™ H4 Hybrid Multi-Mode Microplate Reader [Internet]. 2010.
751 http://www.biotek.com

752 23. Love MI, Huber W, Anders S. Moderated estimation of fold change and dispersion
753 for RNA-seq data with DESeq2. *Genome Biol*. 2014;15.
754 http://dx.doi.org/10.1186/s13059-014-0550-8
755 24. Ge SX, Son EW, Yao R. iDEP: An integrated web application for differential
756 expression and pathway analysis of RNA-Seq data. *BMC Bioinformatics* 2018;19.
757 http://dx.doi.org/10.1186/s12859-018-2486-6
758 25. Baecker V. ImageJ Macro Tool Sets for Biological Image Analysis. Conference
759 26. Kanehisa M, Sato Y. KEGG Mapper for inferring cellular functions from protein
760 sequences. *Protein Sci.* 2020;29:28–35.
761 27. Mi H, Huang X, Muruganujan A, Tang H, Mills C, Kang D, Thomas PD. PANTHER
762 version 14: more genomes, a new PANTHER GO-slim and improvements in
763 enrichment analysis tools. *Nucleic Acids Res.* 2019;47(D1):D419-D426.
764 28. Therneau T. A Package for Survival Analysis in R. R package version 3.4-0
765 [Internet]. 2022. https://CRAN.R-project.org/package=survival
766 29. Kassambara, A., Kosinski, M., & Biecek, F. S.Package “survminer” Type Package
767 Title Drawing Survival Curves using “ggplot2;” 2022
768 30. Wickham H. Ggplot2 : elegant graphics for data analysis. Springer; 2009.
769 31. Love, M. I., Huber, W., & Anders, S. Moderated estimation of fold change and
770 dispersion for RNA-seq data with DESeq2. *Genome Biology* 2014; *15*(12).
771 https://doi.org/10.1186/s13059-014-0550-8
772 32. Kolde R. pheatmap: Pretty Heatmaps. R package version 1.0.12 [Internet]. 2019.
773 Available from: https://CRAN.R-project.org/package=pheatmap

774 33. Frank M, Harrell E. Hmisc: A package of miscellaneous R functions [Internet]. 2020.
775 Available from: http://biostat.mc.vanderbilt.edu/Hmisc
776 34. Urbanek S, Johnson K. tiff: Read and Write TIFF Images. R package version 0.1-
777 11. 2020; Available from: https://CRAN.R-project.org/package=tiff
778 35. Jia Y, Xie J. Promising molecular mechanisms responsible for gemcitabine
779 resistance in cancer. *Genes and Diseases* 2015;2(4):299-306.
780 http://dx.doi.org/10.1016/j.gendis.2015.07.003
781 36. Wei X, Zhou X, Zhao Y, He Y, Weng Z, Xu C. A 14-gene gemcitabine resistance
782 gene signature is significantly associated with the prognosis of pancreatic cancer
783 patients. *Sci Rep* 2021;11(6087). http://dx.doi.org/10.1038/s41598-021-85680-x
784 37. Akada M, Crnogorac-Jurcevic T, Lattimore S, Mahon P, Lopes R, Sunamura M, et
785 al. Intrinsic Chemoresistance to Gemcitabine Is Associated with Decreased
786 Expression of BNIP3 in Pancreatic Cancer. *Clin Cancer Res.* 2005;11(8):3094-101.
787 https://aacrjournals.org/clincancerres/article/11/8/3094/188241/Intrinsic-
788 Chemoresistance-to-Gemcitabine-Is
789 38. Nakano Y, Tanno S, Koizumi K, Nishikawa T, Nakamura K, Minoguchi M, et al.
790 Gemcitabine chemoresistance and molecular markers associated with gemcitabine
791 transport and metabolism in human pancreatic cancer cells. *Br J Cancer*
792 2007;96:457–63.
793 39. Vasaikar SV, Deshmukh AP, den Hollander P, Addanki S, Kuburich NA, Kudaravalli
794 S, Joseph R, Chang JT, Soundararajan R, Mani SA. EMTome: a resource for pan-
795 cancer analysis of epithelial-mesenchymal transition genes and signatures. *Br J*

796 *Cancer*. 2021;124(1):259-269. doi: 10.1038/s41416-020-01178-9. Epub 2020 Dec
797 10. PMID: 33299129; PMCID: PMC7782839.
798 40. Huang L, Jansen L, Balavarca Y, Babaei M, van der Geest L, Lemmens V, Van
799 Eycken L, De Schutter H, Johannesen TB, Primic-Žakelj M, Zadnik V,
800 Besselink MG, Schrotz-King P, Brenner H. Stratified survival of resected and
801 overall pancreatic cancer patients in Europe and the USA in the early twenty-
802 first century: a large, international population-based study. BMC Med. 2018
803 Aug 21;16(1):125. doi: 10.1186/s12916-018-1120-9. PMID: 30126408;
804 PMCID: PMC6102804.
805 41. Ghanem NZ, Matter ML, Ramos JW. Regulation of Leukaemia Associated Rho
806 GEF (LARG/ARHGEF12). *Small GTPases* 2022;13(1)196-204;
807 http://dx.doi.org/10.1080/21541248.2021.1951590
808 42. Lin, J., Xu, Z., Xie, J., Deng, X., Jiang, L., Chen, H., Peng, C., Li, H., Zhang, J., &
809 Shen, B. Oncogene APOL1 promotes proliferation and inhibits apoptosis via
810 activating NOTCH1 signaling pathway in pancreatic cancer. *Cell Death and*
811 *Disease*; 2021; 12(8). https://doi.org/10.1038/s41419-021-03985-1
812 43. Cruz-Monserrate Z, Qiu S, Evers BM, O'Connor KL. Upregulation and redistribution
813 of integrin α6β4 expression occurs at an early stage in pancreatic adenocarcinoma
814 progression. *Mod Pathol*. 2007;20:656–67.
815 44. Duchateau PN, Pullinger CR, Orellana RE, Kunitake ST, Naya-Vigne J, O'Connor
816 PM, et al. Apolipoprotein L, a new human high density lipoprotein apolipoprotein
817 expressed by the pancreas. Identification, cloning, characterization, and plasma
818 distribution of apolipoprotein L. *J Biol Chem.* 1997;272:25576–82.

819 45. Cho S, Lu M, He X, Ee PLR, Bhat U, Schneider E, et al. Notch1 regulates the
820 expression of the multidrug resistance gene ABCC1/MRP1 in cultured cancer cells.
821 *Proc Natl Acad Sci* 2011;108:20778–83.
822 46. Sangphech N, Keawvilai P, Palaga T. Notch signaling increases PPARγ protein
823 stability and enhances lipid uptake through AKT in IL-4-stimulated THP-1 and
824 primary human macrophages. *FEBS Open Bio.* 2020;10:1082–95.
825 47. Mohanty A, Nam A, Pozhitkov A, Yang L, Srivastava S, Nathan A, et al. A Non-
826 genetic Mechanism Involving the Integrin β4/Paxillin Axis Contributes to
827 Chemoresistance in Lung Cancer. *iScience* 2020;23.
828 http://dx.doi.org/10.1016/j.isci.2020.101496
829 48. Yoshioka T, Otero J, Chen Y, Kim YM, Koutcher JA, Satagopan J, et al. β4 Integrin
830 signaling induces expansion of prostate tumor progenitors. *J Clin Invest*.
831 2013;123:682–99.
832 49. Masugi Y, Yamazaki K, Emoto K, Effendi K, Tsujikawa H, Kitago M, Itano O,
833 Kitagawa Y, Sakamoto M. Upregulation of integrin β4 promotes epithelial-
834 mesenchymal transition and is a novel prognostic marker in pancreatic ductal
835 adenocarcinoma. *Lab Invest.*; 2015;95(3):308-19. doi: 10.1038/labinvest.2014.166.
836 PMID: 25599535.
837 50. Giancotti FG, Ruoslahti E. Integrin signaling. Science. 2017;285:1028–32.
838 51. Meng X, Liu P, Wu Y, Liu X, Huang Y, Yu B, et al. Integrin beta 4 (ITGB4) and its
839 tyrosine-1510 phosphorylation promote pancreatic tumorigenesis and regulate the
840 MEK1-ERK1/2 signaling pathway. *Bosn J Basic Med Sci*. 2020;20:106–16.
841 52. ImageJ User and Developer Conference 2012 At: Luxembourg. 2012.

842

843 **ADDITIONAL FILES**

844 **Additional file 1: Figure S1.pdf**

845 **a)** Kaplan-Meier curve of Recurrence/Disease Free Survival (RFS) using GEPIA PPAD
846 dataset. Log rank p=0.047 **b)** Protein abundance of ANGPTL4 in cell lysate and
847 supernatant as measured by AlphaLISA assay for normalization by cell input.
848 MP2_ANGPTL4_OE vs MP2_ANPGTL4_KD p=0.0075 and 0.0018 (**) for lysate and
849 supernatant. MP2_ANGPTL4_OE vs MP2 p=0.0055 (**) for lysate. **c)** Heatmap of
850 RNA-seq data for 1198 DEG from MP2_ANGPTL4_OE vs MP2_ANGPTL4_KD with
851 thresholds: baseMean>10 padj<0.05, and $\log_2$ fold change +/-0.7.

852

853 **Additional file 2: Figure S2.pdf**

854 **a)** ITGB4 expression measured by qPCR and normalized by the housekeeping gene
855 *ACTB*. All data points are plotted relative to the ANGPTL4_OE line. **b)** *APOL1* expression
856 measured by qPCR and normalized by the housekeeping gene *ACTB*. All data points are
857 plotted relative to the ANGPTL4_OE line. **c)** Cell viability over time normalized to control
858 MP2 cells (lt. pink) at time 0 for MP2_NTC (pink), MP2_ANGPTL4_OE+DsiRNA_NTC
859 (turquoise), MP2_ANGPTL4_OE_ITGB4_KD (lavender), and
860 MP2_ANGPTL4_OE_APOL1_KD (purple).

861

862 **Additional file 3: Table S1.txt**

863 P-values associated with qPCR and viability data

864

865 **Additional file 4: Table S2.txt**

866 DEG from MP2_ANGPTL4_OE vs MP2_ANGPTL4_KD analysis with or without
867 gemcitabine treatment

868

869 **Additional file 5: Table S3.txt**

870 114 Gemcitabine Resistance Genes

871

872 **Additional file 6: Table S4.txt**

873 AMIGO2 Panther GO biological process complete analysis for DEG retrieved from with
874 or without gemcitabine analysis

875

876 **Additional file 7: Table S5.txt**

877 AMIGO2 Panther GO biological process EMT results for with or without gemcitabine
878 analysis

879

880 **Additional file 8: Table S6.txt**

881 List of 42 DEG genes for both ANGPTL4 expression and gemcitabine resistance

882

883 **Additional file 9: Table S7.txt**

884 Correlation analysis of TCGA-PAAD data using DEG gene list from MP2_ANGPTL4_OE
885 vs MP2_ANGPTL4_KD analysis with or without gemcitabine treatment

886

887 **Additional file 10: Table S8.txt**

888 Pathway analysis results from DEG from MP2_ANGPTL4_OE vs MP2_ANGPTL4_KD
889 analysis
890
891 **FIGURE LEGENDS**
892 **Figure 1: Expression of *ANGPTL4* is associated with patient outcomes and**
893 **modifies expression of resistance-associated genes.**
894 **a)** A Kaplan Meier curve for overall survival using TCGA-PAAD data (n=90). Top (red)
895 and bottom (blue) 25% average *ANGPTL4* gene expression are significantly different.
896 (p=0.043, log-rank test) **b)** Relative expression of ANGPTL4 transcript in
897 MP2_ANGPTL4_KD (black circles), MP2 (pink squares), and MP2_ANGPTL4_OE
898 (turquoise triangles) as measured by qPCR. P-values from unpaired, two-tailed
899 parametric t-tests performed with 95% confidence intervals are displayed. Values are
900 normalized with *ACTB* as the housekeeper. (P-values ≤ 0.0001=****) **c)** Heatmap
901 displaying RNA-seq results from MP2_ANGPTL4_KD (black), MP2_NTC (pink), and
902 MP2_ANGPTL4_OE (turquoise) cell lines. Displayed are 15 genes associated with both
903 ANGPTL4 overexpression and gemcitabine resistance. Normalized expression for each
904 of the 15 genes is plotted in the heatmap. Red (*) indicate ITGB4 used for later
905 experiments.
906
907 **Figure 2: Gemcitabine resistance signature in PDAC cells with high ANGPTL4**
908 **a)** Cell viability was measured for MP2_ANGPTL4_KD (black), MP2_NTC (pink), and
909 MP2_ANGPTL4_OE (turquoise) cells treated with 0, 5nM, or 12.5nM gemcitabine. A
910 relative viability reflects normalization to cells not treated with gemcitabine. P-value

911 asterisks: ≤0.01=**, ≤0.001=*** & ≤0.0001=****, unpaired, two tailed t-test **b)** Heatmap of

912 gene expression measured by RNA-seq in MP2_ANGPTL4_KD (black/gray), MP2
913 (pink/light pink), and MP2_ANGPTL4_OE (turquoise/aqua) cell lines both untreated and
914 treated with 1.5nM gemcitabine. Normalized expression of the 42 genes that resulted
915 from an intersection of ANGPTL4 expression DEGs and gemcitabine treatment response
916 DEGs are included in the heatmap. **c)** Kaplan-Meier curve for overall survival using
917 TCGA-PAAD data (n=90) where patients were divided into quartiles with highest (red)
918 and lowest (blue) using mean expression of the 42 genes in the intersection (40 genes
919 were available in TCGA: *KDM7a* and *STN1* were omitted). P-values were derived from a
920 log-rank test.

921

922 **Figure 3: ITGB4 and APOL1 inhibition sensitizes cells overexpressing ANGPTL4 to**
923 **gemcitabine.**

924 **a-b)** Kaplan-Meier plot for overall survival using TCGA-PAAD data. Patients (n=90) with
925 top (red) and bottom (blue) 25% average *ANGPTL4* gene expression and *APOL1* or
926 *ITGB4* gene expression (p=0.01 and p=0.014, respectively, log-rank test). **c)** ANGPTL4
927 expression measured by qPCR normalized to MP2_ANGPTL4_OE+DsiRNA_NTC
928 (turquoise) control: MP2 (pink), MP2_ANGPTL4_OE_ITGB4_KD (lavender), and
929 MP2_ANGPTL4_OE_APOL1_KD (purple) compared to mean of
930 MP2_ANGPTL4_OE+DsiRNA_NTC (MP2_ANGPTL4_OE cells transduced with non-
931 targeting control siRNA). Expression is normalized to the housekeeping gene *ACTB*. P-

932 values ≤ 0.0001=****; unpaired two-tailed parametric t-test **d)** Relative viability is plotted

933 by normalizing all data to cells not treated with gemcitabine. MP2_ANGPTL4_KD (black),
934 MP2_NTC (pink), MP2_ANGPTL4_OE+DsiRNA_NTC (turquoise),
935 MP2_ANGPTL4_OE_ITGB4_KD (lavender), and MP2_ANGPTL4_OE_APOL1_KD
936 (purple) cells treated with 0, 5nM, or 12.5nM gemcitabine. Sample size ranges from 4-
937 11 per condition. P-value asterisks: ≤0.001=*** & ≤0.0001=****, unpaired, two-tailed
938 parametric t-tests.
939
940 **Figure 4: ANGPTL4 overexpression correlation with EMT.**
941 **a)** Pathway analysis of 1198 DEG revealed common cancer pathways. Red=$\log_2$FC >0.7
942 and Blue=$\log_2$FC <0.7. **b)** Wound healing assay results at 0 hrs (after initial wound) and
943 48 hours MP2_NTC (pink), MP2_ANGPTL4_OE+DsiRNA_NTC (turquoise),
944 MP2_ANGPTL4_OE_ITGB4_KD (lavender), and MP2_ANGPTL4_OE_APOL1_KD
945 (purple). Each set was performed in triplicate or quadruplicate. **c)** Time to close half the
946 half the gap (t1/2 gap) for each of the four cell types is plotted. t1/2: MP2=57.7hrs,
947 MP2_ANGPTL4_OE= 31.6 hrs., MP2_ANGPTL4_OE_ITGB4_KD= 192 hrs., and
948 MP2_ANGPTL4_OE_APOL1_KD=52.96 hrs. P-values ≤0.01=**, unpaired parametric t-
949 test

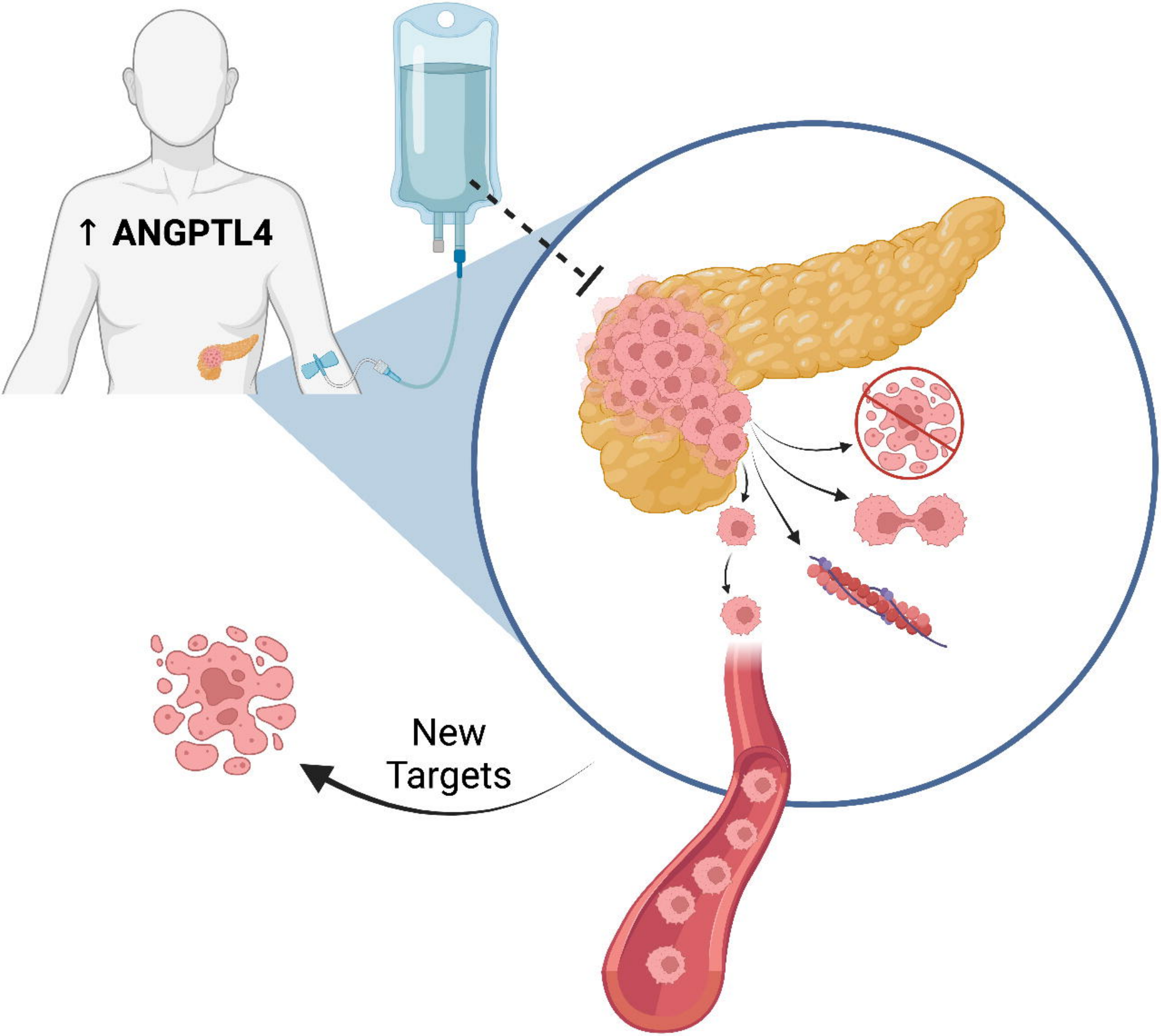
↑ ANGPTL4
New
Targets

Figure 4

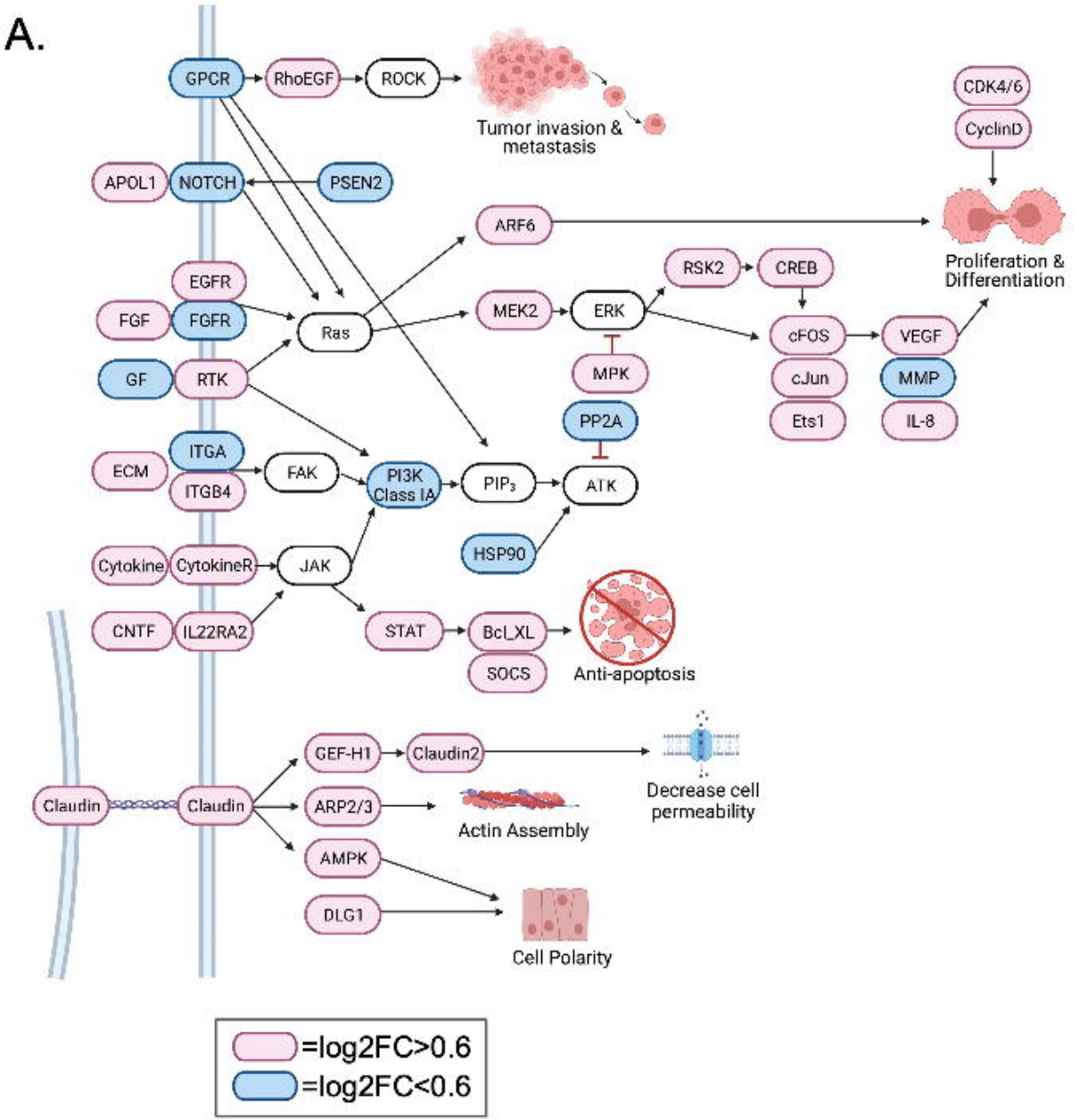
A.
GPCR
RhoEGF
ROCK
Tumor invasion & metastasis
CDK4/6
CyclinD
APOL1
NOTCH
PSEN2
ARF6
Proliferation & Differentiation
EGFR
FGF
FGFR
Ras
MEK2
ERK
RSK2
CREB
cFOS
VEGF
GF
RTK
MPK
cJun
MMP
PP2A
Ets1
IL-8
ITGA
ECM
ITGB4
FAK
PI3K Class IA
PIP3
ATK
HSP90
Cytokine
CytokineR
JAK
CNTF
IL22RA2
STAT
Bcl_XL
SOCS
Anti-apoptosis
Claudin
Claudin
GEF-H1
Claudin2
Decrease cell permeability
ARP2/3
Actin Assembly
AMPK
DLG1
Cell Polarity
=log2FC>0.6
=log2FC<0.6

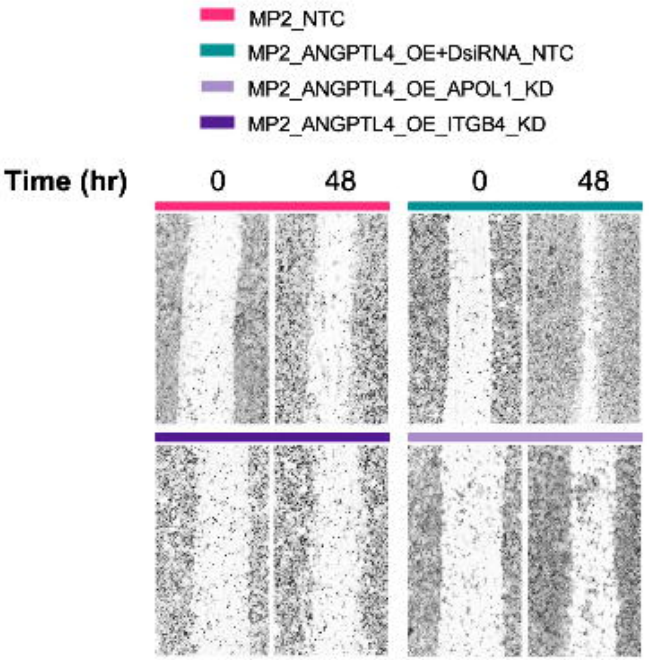
B.
MP2_NTC
MP2_ANGPTL4_OE+DsiRNA_NTC
MP2_ANGPTL4_OE_APOL1_KD
MP2_ANGPTL4_OE_ITGB4_KD
Time (hr)
0
48
0
48

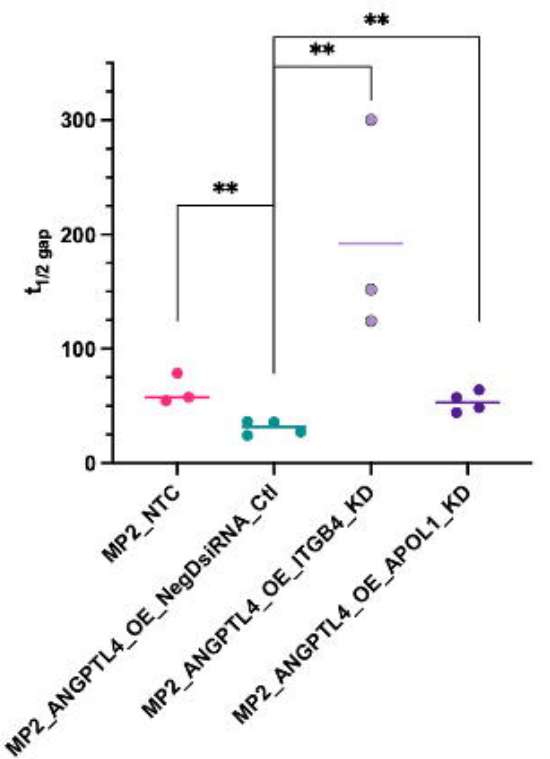
C.
t1/2 gap
300
200
100
0
**
**
**
MP2_NTC
MP2_ANGPTL4_OE_NegDsiRNA_Ctl
MP2_ANGPTL4_OE_ITGB4_KD
MP2_ANGPTL4_OE_APOL1_KD

Figure 3

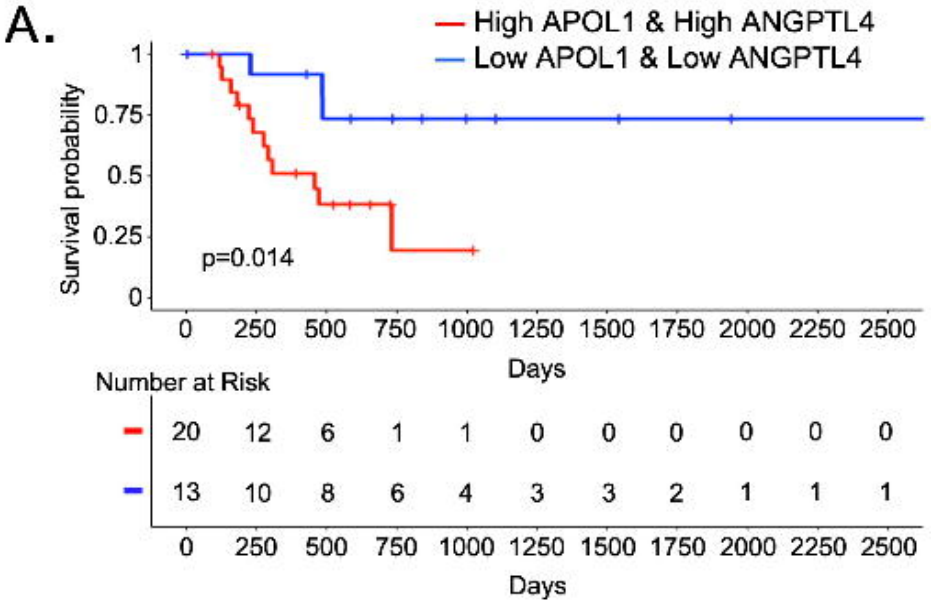
A.
High APOL1 & High ANGPTL4
Low APOL1 & Low ANGPTL4
Survival probability
1
0.75
0.5
0.25
0
p=0.014
0 250 500 750 1000 1250 1500 1750 2000 2250 2500
Days
Number at Risk
20 12 6 1 1 0 0 0 0 0 0
13 10 8 6 4 3 3 2 1 1 1
0 250 500 750 1000 1250 1500 1750 2000 2250 2500
Days

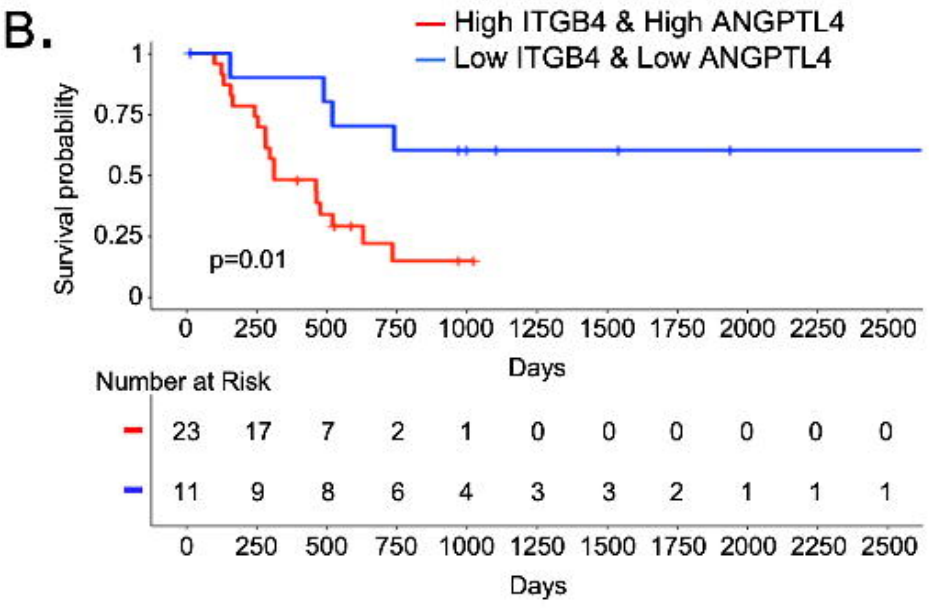
B.
High ITGB4 & High ANGPTL4
Low ITGB4 & Low ANGPTL4
Survival probability
1
0.75
0.5
0.25
0
p=0.01
0 250 500 750 1000 1250 1500 1750 2000 2250 2500
Days
Number at Risk
23 17 7 2 1 0 0 0 0 0 0
11 9 8 6 4 3 3 2 1 1 1
0 250 500 750 1000 1250 1500 1750 2000 2250 2500
Days

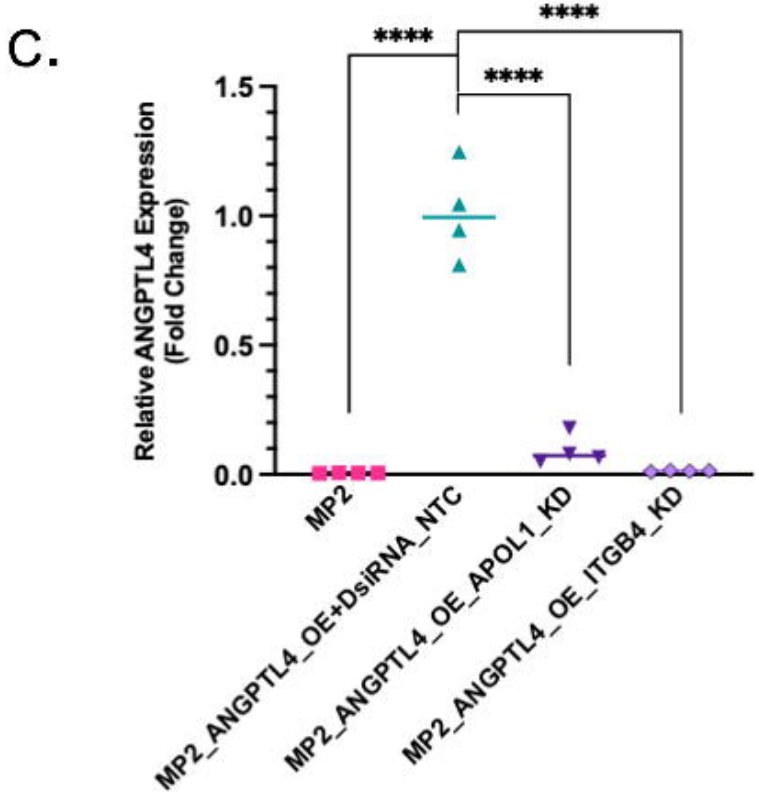
C.
Relative ANGPTL4 Expression (Fold Change)
1.5
1.0
0.5
0.0
****
****
****
MP2
MP2_ANGPTL4_OE+DsiRNA_NTC
MP2_ANGPTL4_OE_APOL1_KD
MP2_ANGPTL4_OE_ITGB4_KD

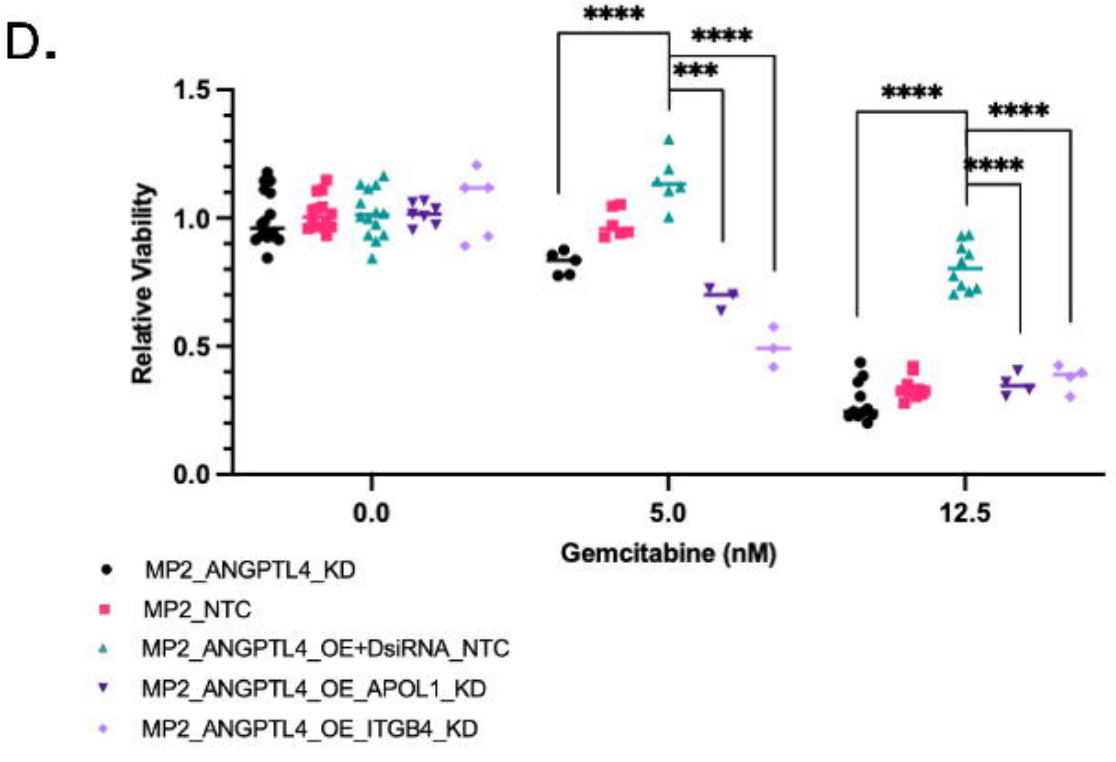
D.
Relative Viability
1.5
1.0
0.5
0.0
****
****
***
****
****
****
****
0.0
5.0
12.5
Gemcitabine (nM)
MP2_ANGPTL4_KD
MP2_NTC
MP2_ANGPTL4_OE+DsiRNA_NTC
MP2_ANGPTL4_OE_APOL1_KD
MP2_ANGPTL4_OE_ITGB4_KD

Figure 1

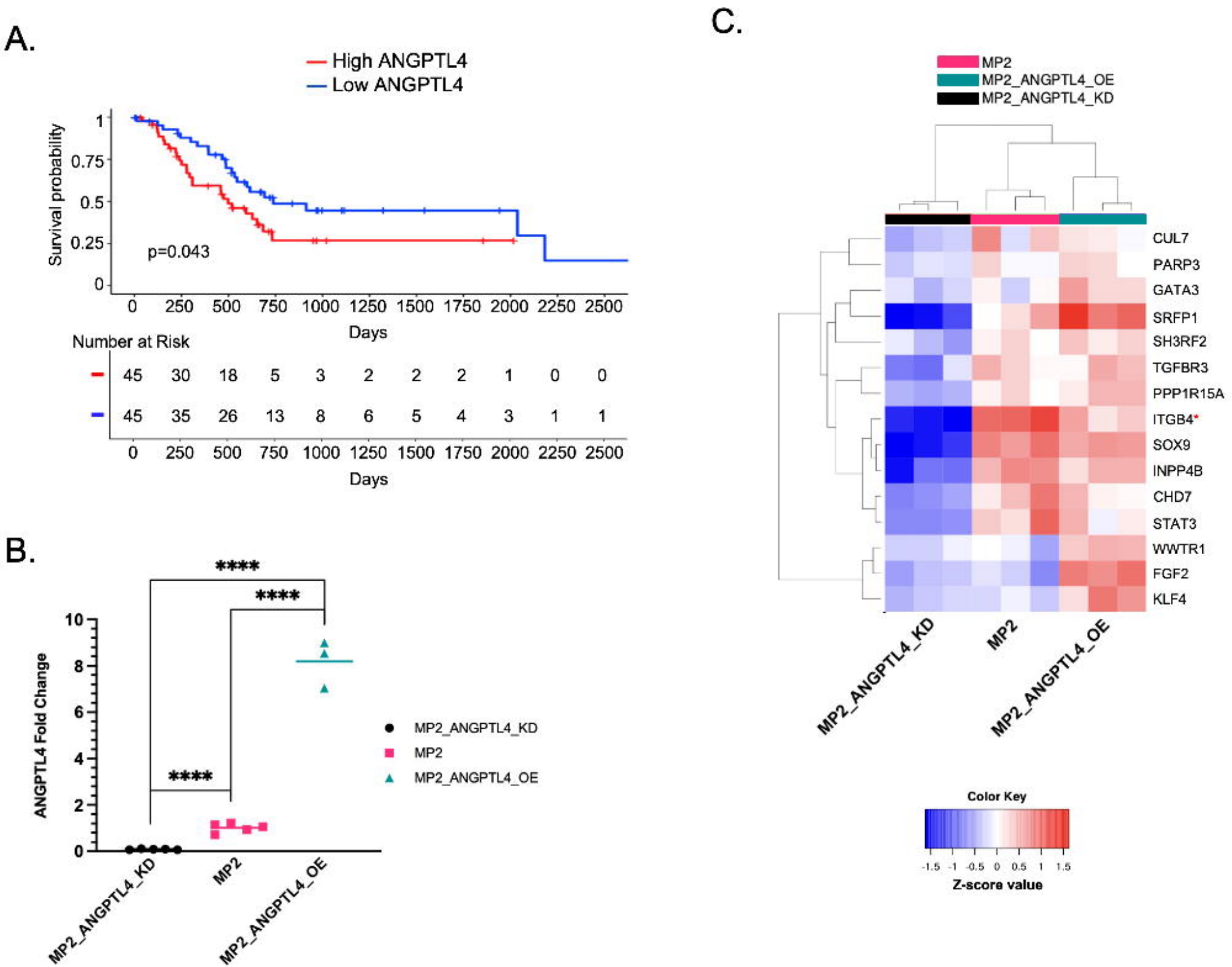
A.
High ANGPTL4
Low ANGPTL4
Survival probability
1
0.75
0.5
0.25
0
p=0.043
0 250 500 750 1000 1250 1500 1750 2000 2250 2500
Days
Number at Risk
45 30 18 5 3 2 2 2 1 0 0
45 35 26 13 8 6 5 4 3 1 1
0 250 500 750 1000 1250 1500 1750 2000 2250 2500
Days
B.
****
****
****
ANGPTL4 Fold Change
10
8
6
4
2
0
MP2_ANGPTL4_KD
MP2
MP2_ANGPTL4_OE
MP2_ANGPTL4_KD
MP2
MP2_ANGPTL4_OE
C.
MP2
MP2_ANGPTL4_OE
MP2_ANGPTL4_KD
CUL7
PARP3
GATA3
SRFP1
SH3RF2
TGFBR3
PPP1R15A
ITGB4*
SOX9
INPP4B
CHD7
STAT3
WWTR1
FGF2
KLF4
MP2_ANGPTL4_KD
MP2
MP2_ANGPTL4_OE
Color Key
-1.5 -1 -0.5 0 0.5 1 1.5
Z-score value

Figure 2

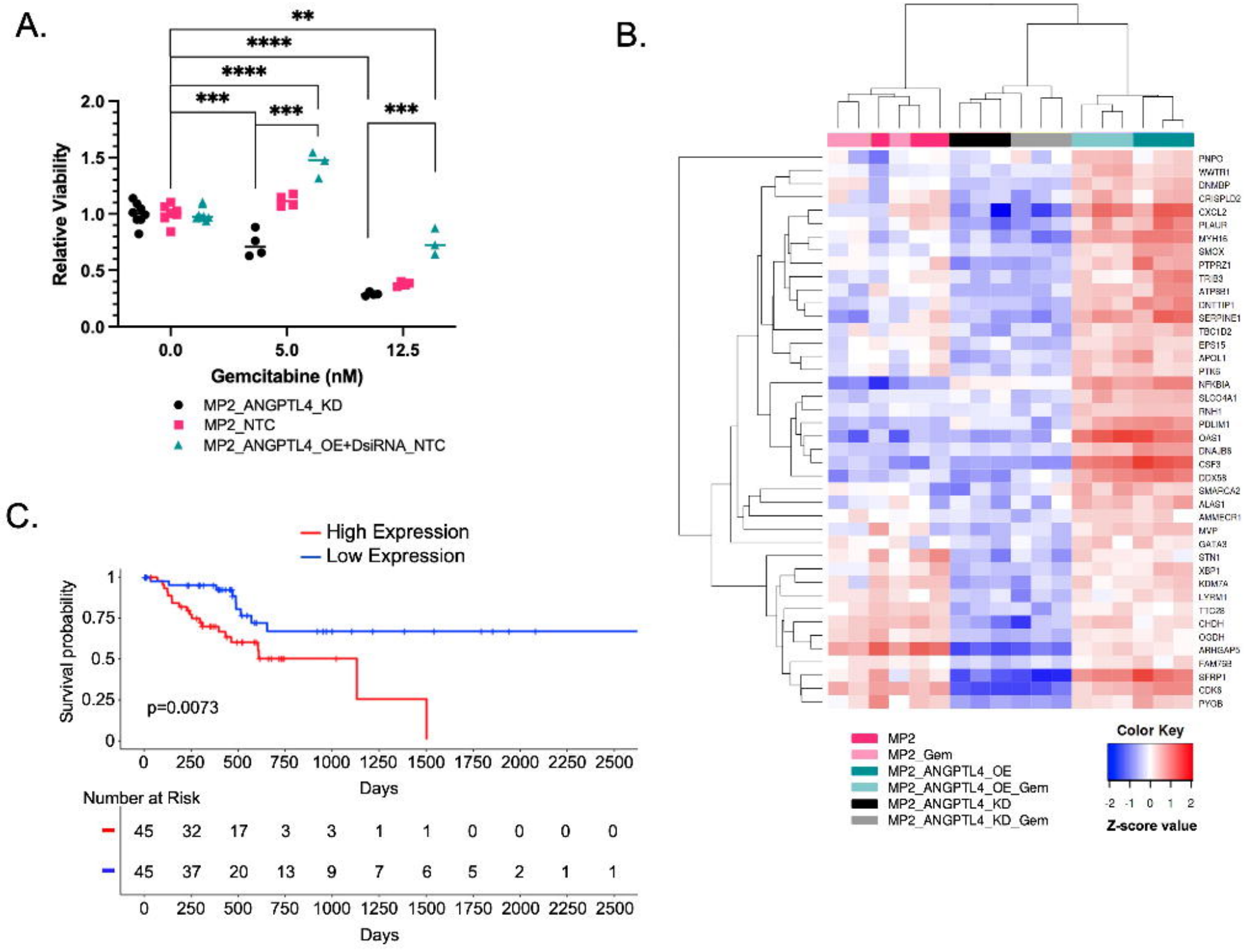
A.
**
****
****
***
***
***
Relative Viability
2.0
1.5
1.0
0.5
0.0
0.0
5.0
12.5
Gemcitabine (nM)
MP2_ANGPTL4_KD
MP2_NTC
MP2_ANGPTL4_OE+DsiRNA_NTC
B.
PNPO
WWTR1
DNMBP
CRISPLD2
CXCL2
PLAUR
MYH16
SMOX
PTPRZ1
TRIB3
ATP8B1
CNTTIP1
SERPINE1
TBC1D2
EPS15
APOL1
PTK6
NFKBIA
SLC04A1
RNH1
PDLIM1
OAS1
DNAJB6
CSF3
COX5B
SMARCA2
ALAS1
AMMECR1
MVP
GATA3
STN1
XBP1
KDM7A
LYRM1
TTC28
CHDH
OGDH
ARHGAP5
FAM72B
SFRP1
CDK8
PYGB
MP2
MP2_Gem
MP2_ANGPTL4_OE
MP2_ANGPTL4_OE_Gem
MP2_ANGPTL4_KD
MP2_ANGPTL4_KD_Gem
Color Key
-2 -1 0 1 2
Z-score value
C.
High Expression
Low Expression
Survival probability
1
0.75
0.5
0.25
0
p=0.0073
0 250 500 750 1000 1250 1500 1750 2000 2250 2500
Days
Number at Risk
45 32 17 3 3 1 1 0 0 0 0
45 37 20 13 9 7 6 5 2 1 1
0 250 500 750 1000 1250 1500 1750 2000 2250 2500
Days